Low-Dose Dose-Response for *In Vitro Nrf*2-ARE Activation in Human Liver HepG2 Cells

Ken Bogen, DrPH, DABT
kbogen@exponent.com

International Dose-Response Society 2017 Annual Meeting
Amherst, MA
April 18–19, 2017

Intracellular Redox Homeostasis

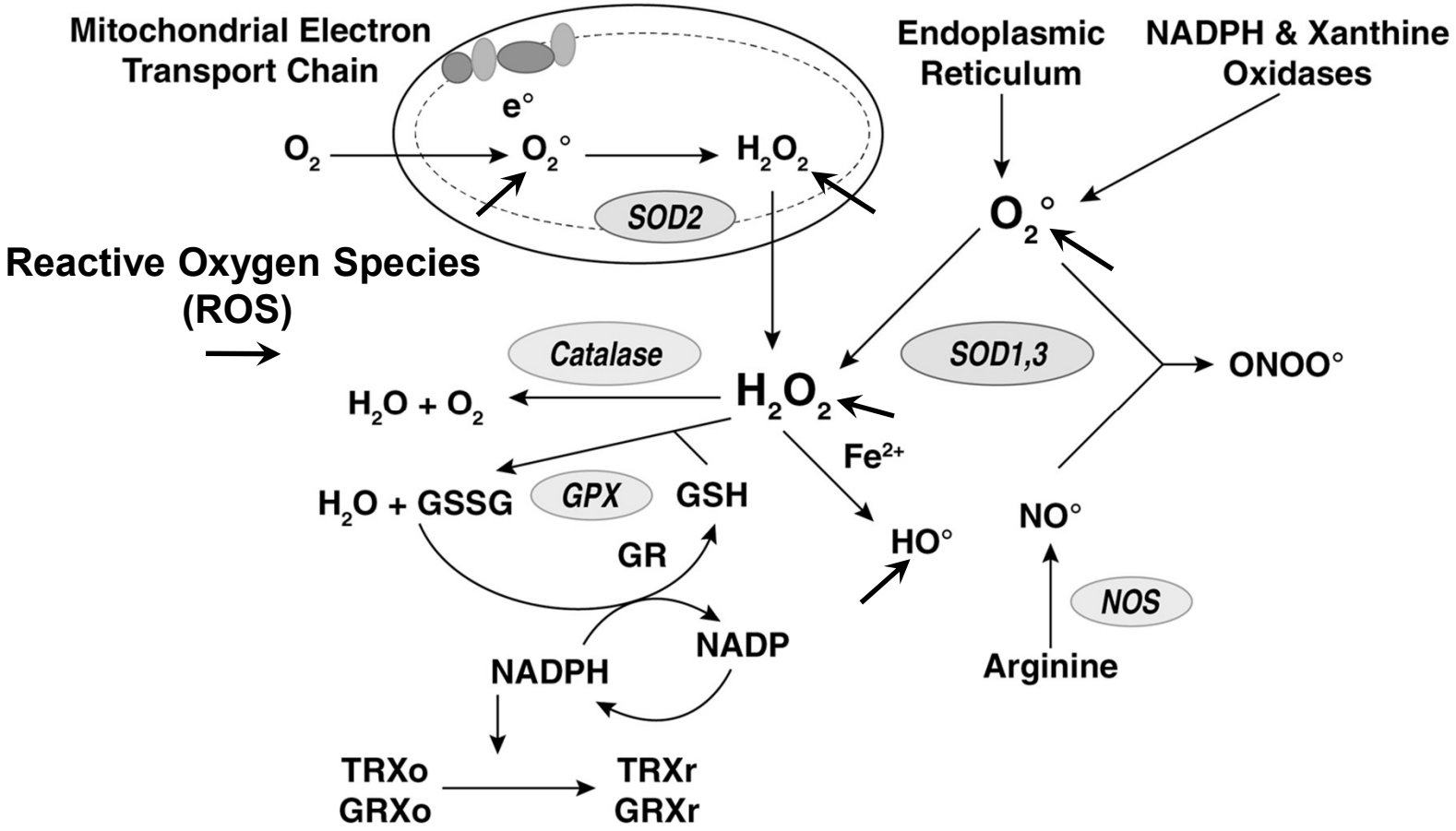

Source: Adapted from Trachootham et al. *Antiox Redox Signal* 2008; 10(8):1343–74.

Redox-sensitive signaling pathways regulate cell survival

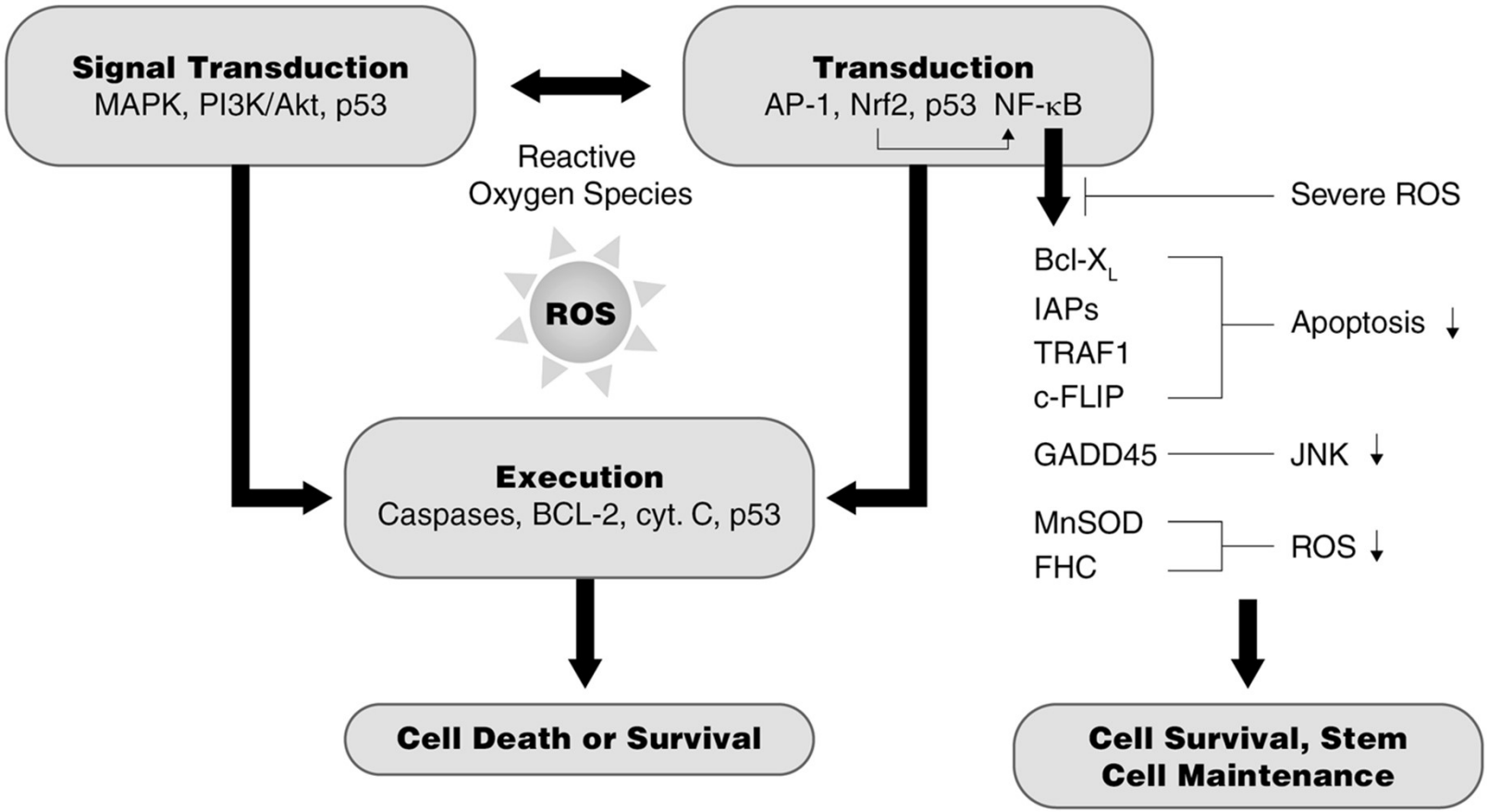

Source: Adapted from Trachootham et al. *Antiox Redox Signal* 2008; 10(8):1343–74.

Redox-sensitive signaling pathways regulate cell survival

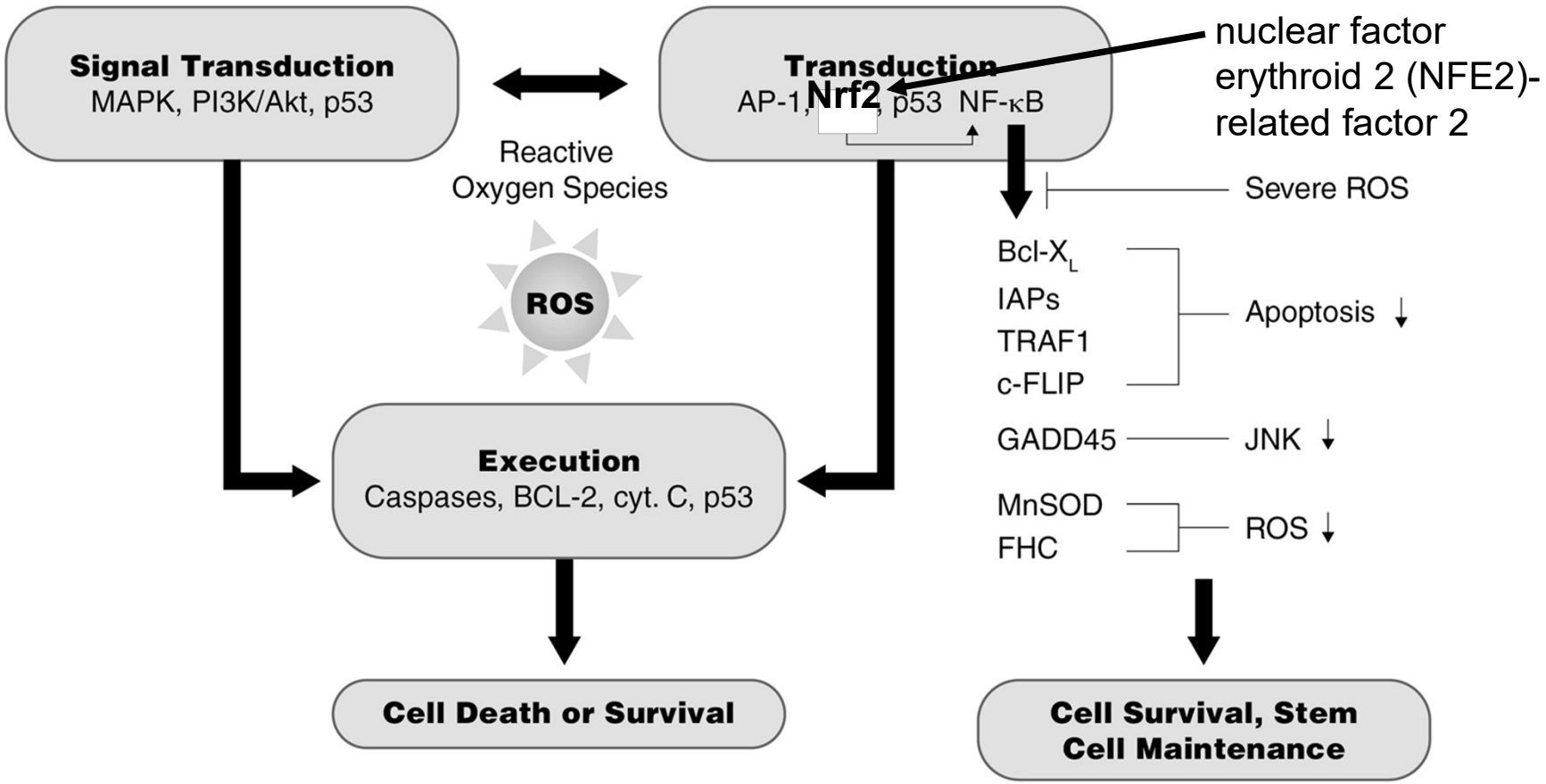

Source: Adapted from Trachootham et al. *Antiox Redox Signal* 2008; 10(8):1343–74.

Keap1 and Nrf2 mediate the activation of the Anti-Oxidant Response Element (ARE)

- Under **basal conditions**, Nrf2 is sequestered in the cytosol by a Keap1 homodimer, which facilitates Nrf2 ubiquitination and proteasomal degradation

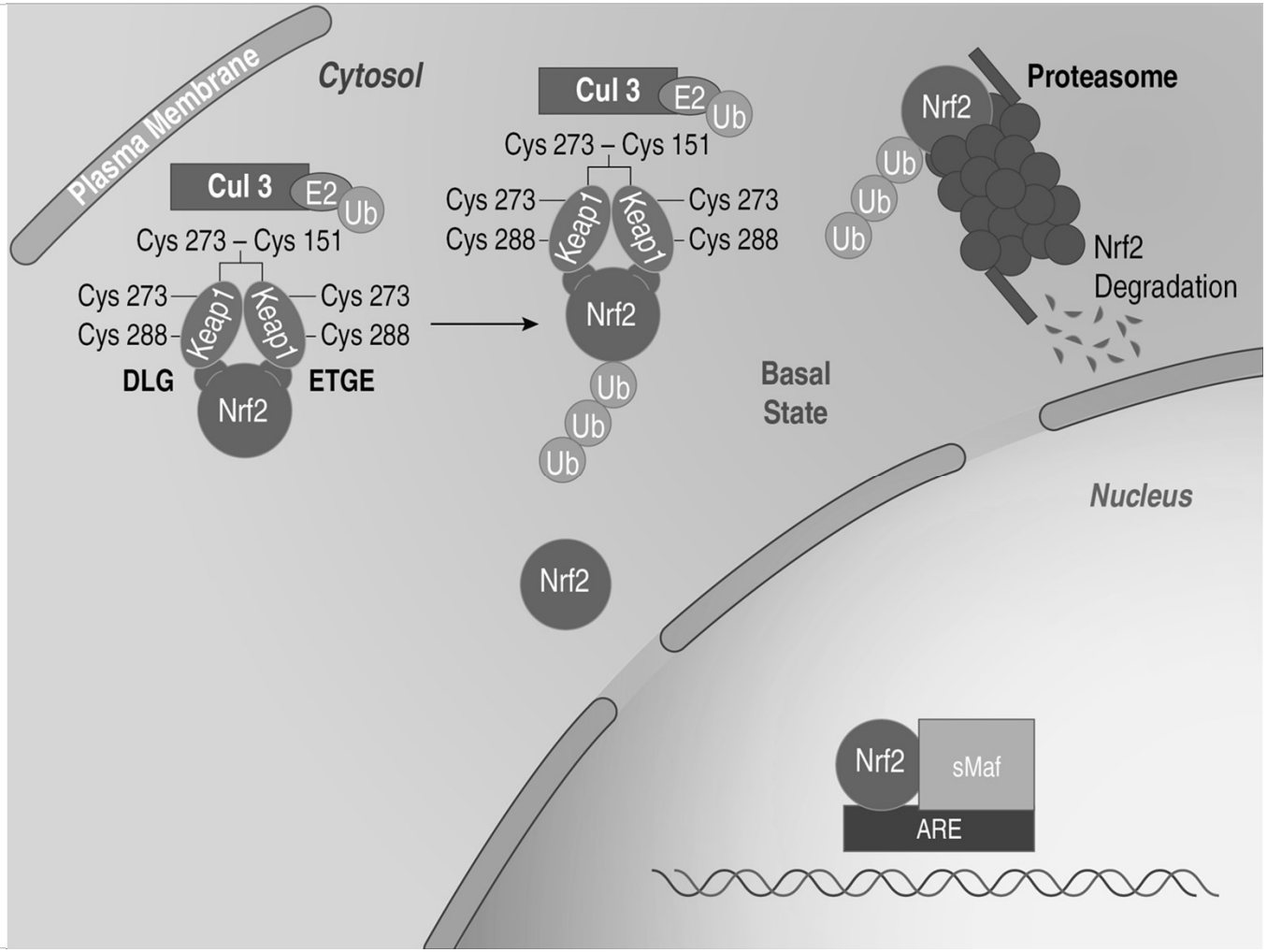

Source: Adapted from: Espinosa-Diez et al. *Redox Biol* 2015; 6:183–97.

Keap1 and Nrf2 mediate the activation of the Anti-Oxidant Response Element (ARE)

- Under basal conditions, Nrf2 is sequestered in the cytosol by a Keap1 homodimer, which facilitates Nrf2 ubiquitination and proteasomal degradation
- **ROS-oxidation** of key Keap1-cysteine residues causes Nrf2 release, allowing it to enter the nucleus and activate the anti-oxidant response element (ARE)

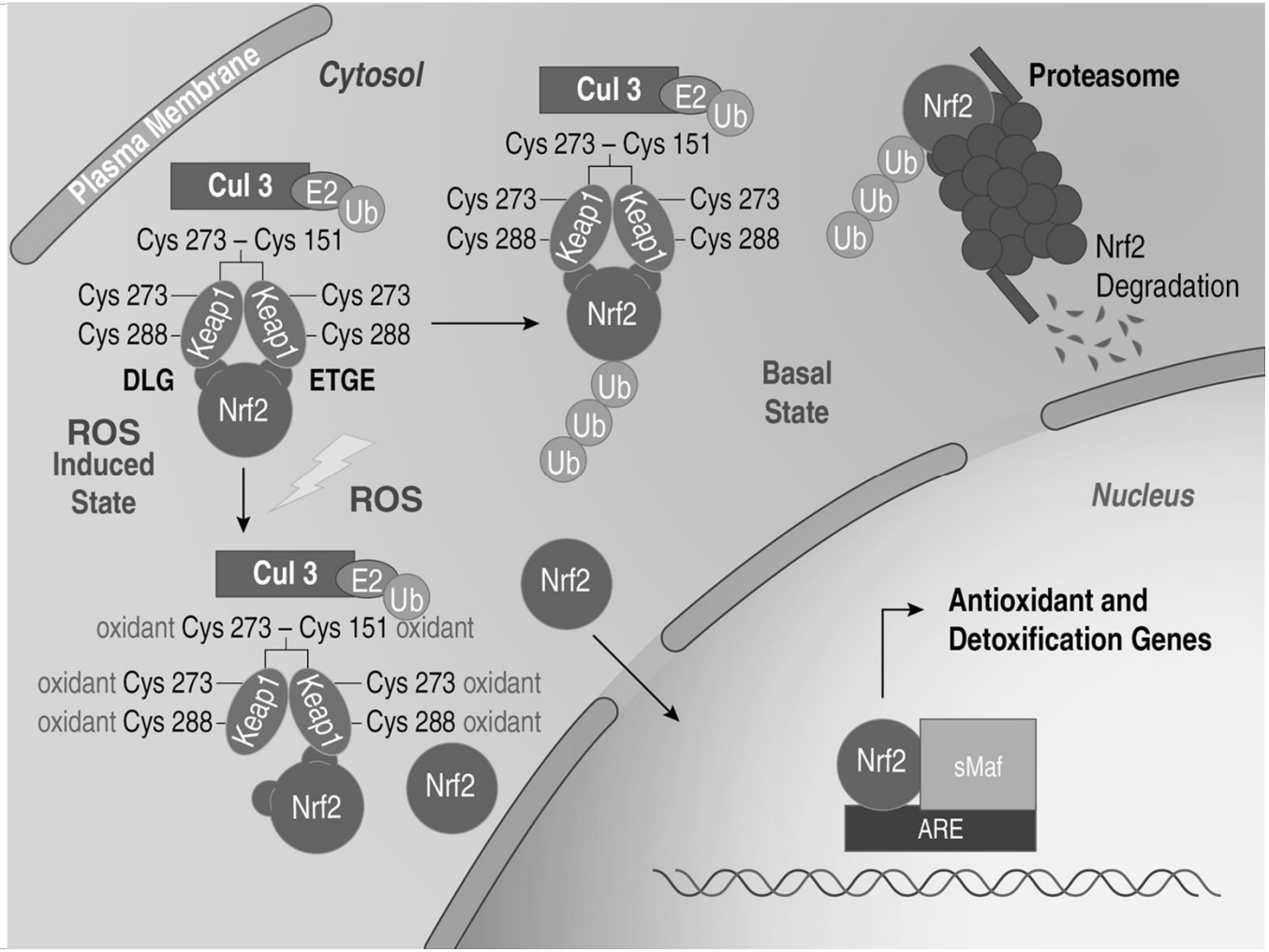

Source: Adapted from: Espinosa-Diez et al. *Redox Biol* 2015; 6:183–97.

Keap1 and Nrf2 mediate the activation of the Anti-Oxidant Response Element (ARE)

- Under basal conditions, Nrf2 is sequestered in the cytosol by a Keap1 homodimer, which facilitates Nrf2 ubiquitination and proteasomal degradation
- **CDDO-Im** binds to Keap1, activating Nrf2 by releasing it from Keap1 and allowing it to enter the nucleus and activate the anti-oxidant response element (ARE)

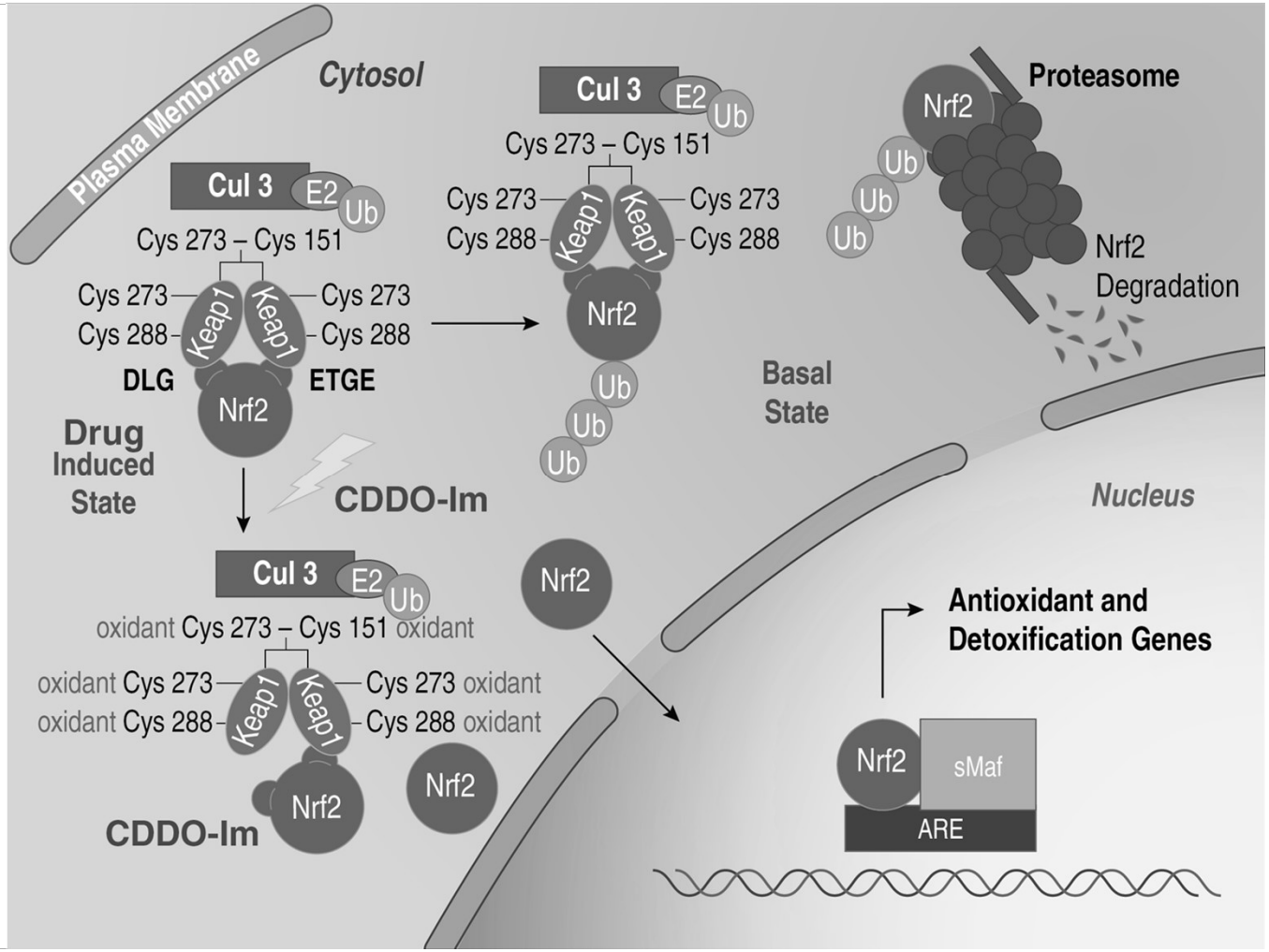

Source: Adapted from: Espinosa-Diez et al. *Redox Biol* 2015; 6:183–97.

Data inconsistent with MSM theory predictions

A team at Dartmouth and Johns Hopkins exposed rats to the potently mutagenic liver carcinogen AFB_1 for 4 weeks, with or without co-administering one of the most potent anti-inflammatory agents (CDDO-Im)

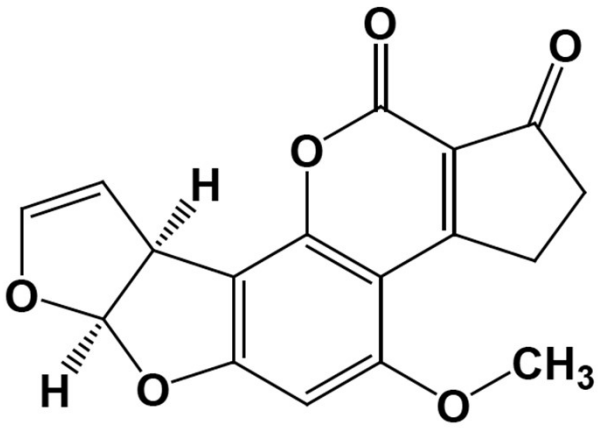

Aflatoxin B_1 (AFB_1)

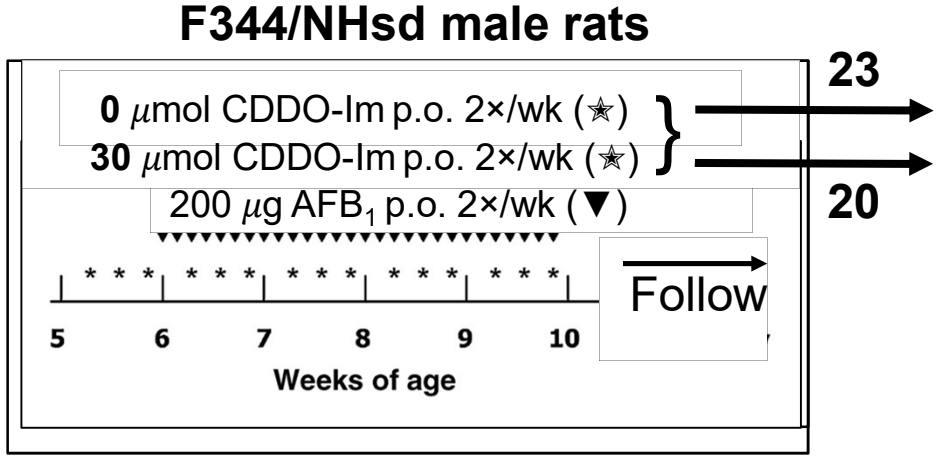

Source: Johnson et al. *Cancer Prev Res* 2014; 7(7):658–665.

Liver DNA Adducts

- N7-guanine (~30/mutation)
- FAPyr (~3/mutation)

Liver foci

Liver tumors

Data inconsistent with MSM theory predictions

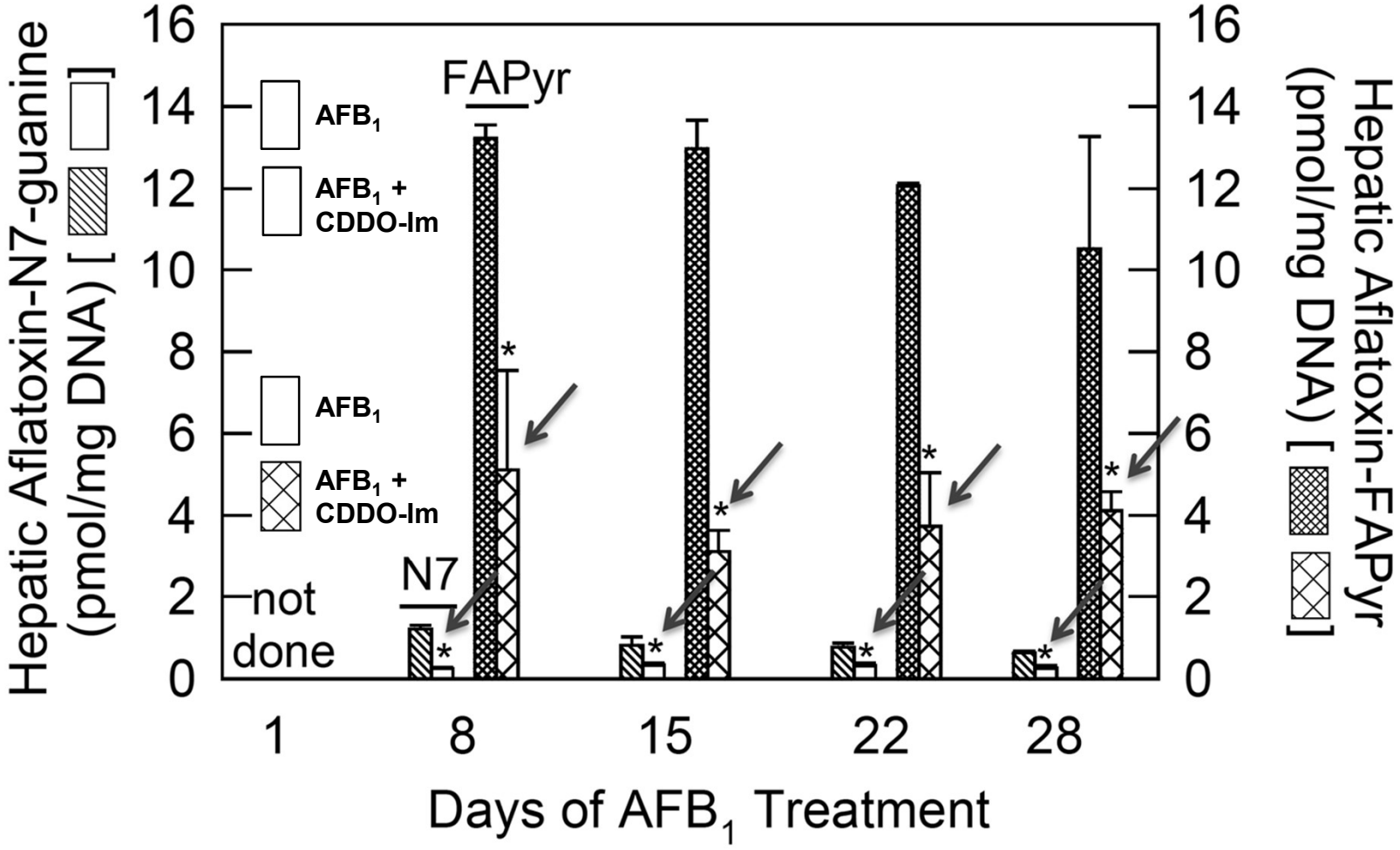

Source: Johnson et al. *Cancer Prev Res* 2014; 7(7):658-665 (via Dr. Bill Roebuck).

Data inconsistent with MSM theory predictions

Treatment	Days of AFB_1	Number of rats	Focal volume % Mean (range)
None	0[a]	3	0
AFB_1	8	3	0.01 (0 - 0.04)
	15	3	0.25 (0.10 - 0.34)
	22	3	3.22 (1.89 - 5.86)
	28	6	13.81 (5.25 - 23.11)
AFB1 + CDDO-Im	8	3	0
	15	3	0
	22	3	0.02 (0 - 0.064)
	28	4	0.01 (0 - 0.02)

[a]Evaluated at day 28

Source: Johnson et al. *Cancer Prev Res* 2014; 7(7):658-665 (via Dr. Bill Roebuck).

Data inconsistent with MSM theory predictions

Consis-tency with MSM expecta-tion if FAPyr adducts cause tumors

Treatment	Days of AFB_1	Number of rats	Focal volume % Mean (range)
None	0[a]	3	0
AFB_1	8	3	0.01 (0 - 0.04)
	15	3	0.25 (0.10 - 0.34)
	22	3	3.22 (1.89 - 5.86)
	28	6	13.81 (5.25 - 23.11)
AFB1 + CDDO-Im	8	3	0
	15	3	0
	22	3	0.02 (0 - 0.064)
	28	4	0.01 (0 - 0.02)

[a]Evaluated at day 28

***p = 0.0095**

Source: Johnson et al. *Cancer Prev Res* 2014; 7(7):658-665 (via Dr. Bill Roebuck).

Data inconsistent with MSM theory predictions

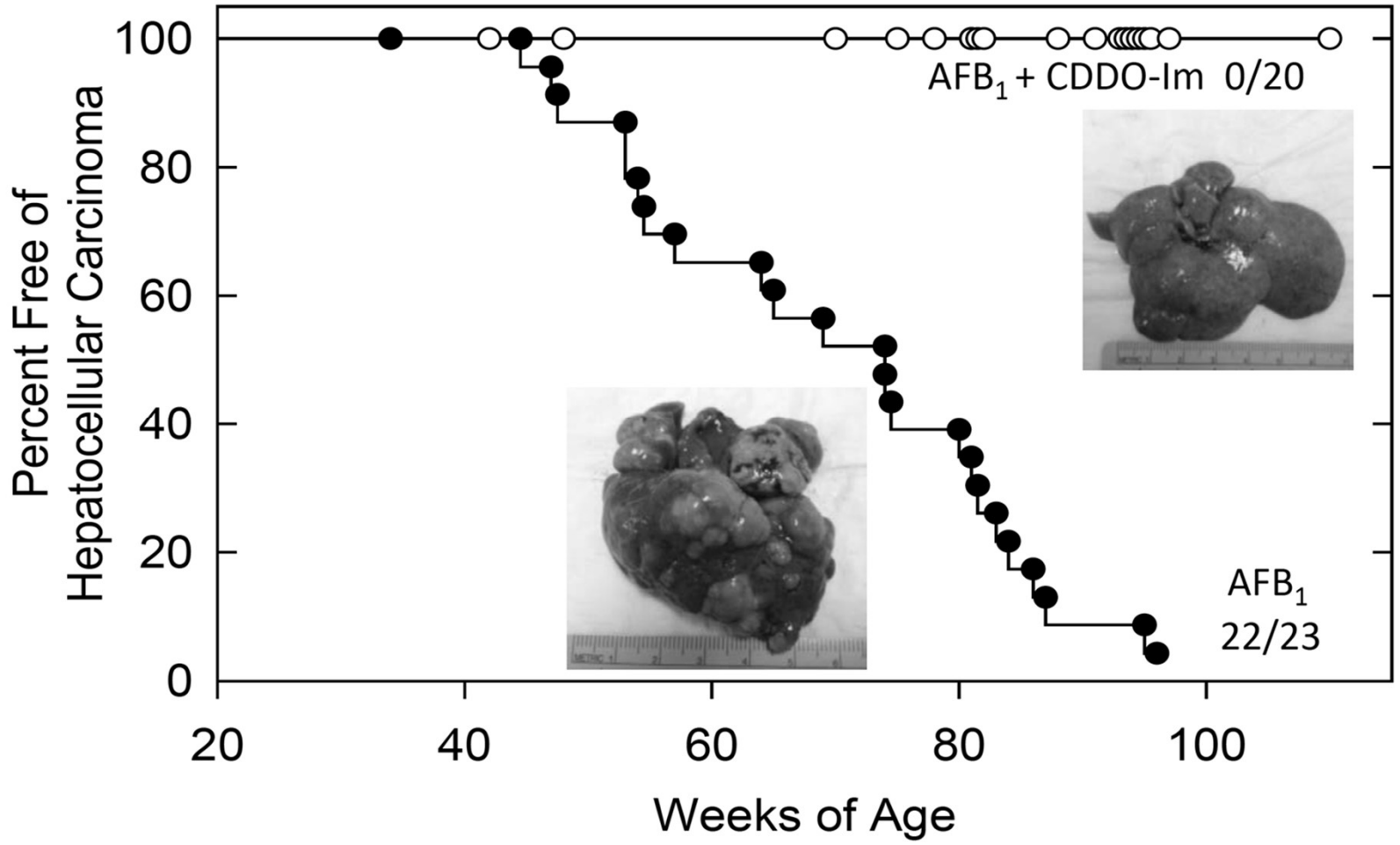

Source: Johnson et al. *Cancer Prev Res* 2014; 7(7):658-665 (via Dr. Bill Roebuck).

Data inconsistent with MSM theory predictions

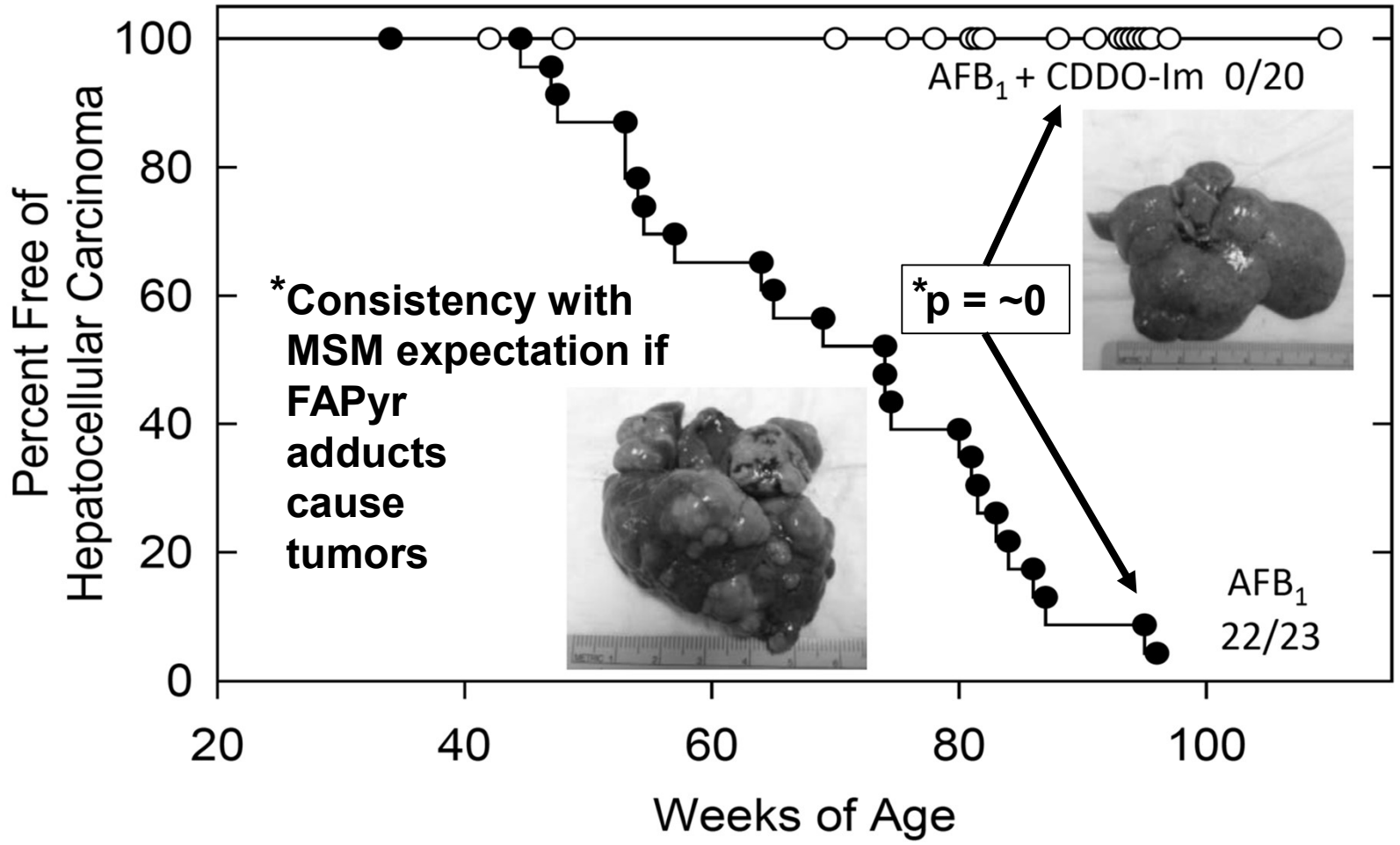

Source: Johnson et al. *Cancer Prev Res* 2014; 7(7):658-665 (via Dr. Bill Roebuck).

Exponent®

Shukla et al. (2012) plotted concentration-response data for Nrf2-ARE activation in Human HepG2 cells

Research

Environ Health Perspect 120:1150–1156 (2012)
http://dx.doi.org/10.1289/ehp.1104709 [Online 2 May 2012]

Profiling Environmental Chemicals for Activity in the Antioxidant Response Element Signaling Pathway Using a High Throughput Screening Approach

Sunita J. Shukla,[1] Ruili Huang,[1] Steven O. Simmons,[2] Raymond R. Tice,[3] Kristine L. Witt,[3] Danielle VanLeer,[1] Ram Ramabhadran,[2] Christopher P. Austin,[1] and Menghang Xia[1]

[1]NIH Chemical Genomics Center, National Institutes of Health, Department of Health and Human Services, Rockville, Maryland, USA; [2]U.S. Environmental Protection Agency, Research Triangle Park, North Carolina, USA; [3]Division of the National Toxicology Program, National Institute of Environmental Health Sciences, National Institutes of Health, Department of Health and Human Services, Research Triangle Park, North Carolina, USA

- **Screened 1,340 chemicals using two assays**
  - ARE *bla* (beta lactamase) cellular reporter
  - ARE *luc* (luciferase) cellular reporter
  - ~3% of all chemicals showed elevated activity
- **Plotted normalized data for 15 chemicals**
- **Obtained plotted data from authors for more detailed fitting and statistical analysis**

Nrf2-ARE activation has a J-shaped dose-response

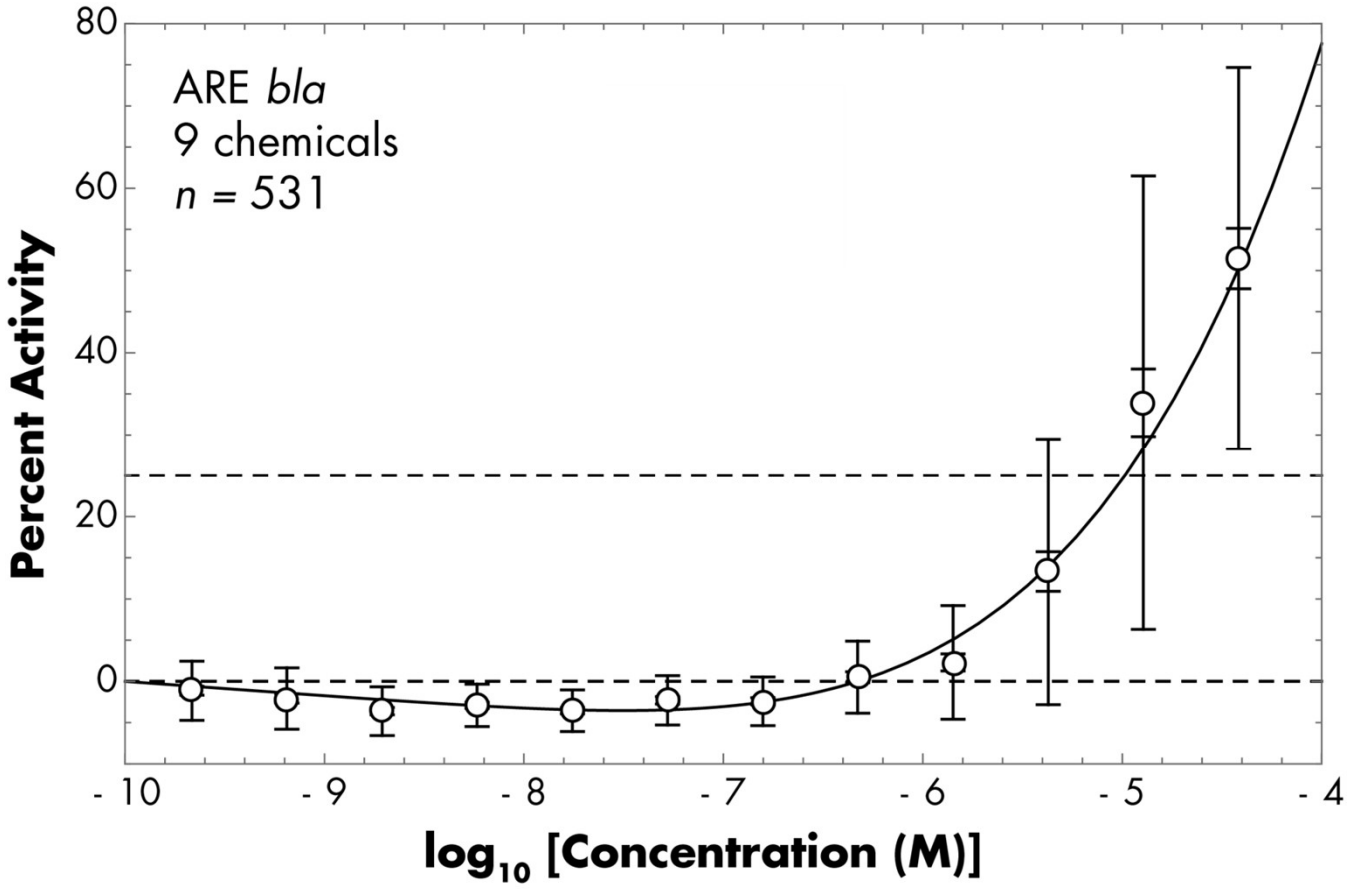

ARE-*bla in vitro* assay response relative to vehicle-exposed controls for Nrf2-ARE-pathway activation at 12 concentrations of 9 hepatotoxic chemicals.

points = arithmetic mean,
inner error bars = ±1 SDM
(outer error bars) = ±1 SD
n = total %-activity data points
dashed horizontal lines = 0%, 25% control

Fit (solid curve, $R^2 = 0.987$) includes an initial linear, **significantly negative slope** ($p = 0.000040$ by 2-tail t-test).

Source: Bogen, Low-dose dose-response for in vitro Nrf2-ARE activation in human HepG2 cells. *Dose-Response* 2017 (*in press*).

Exponent®

Nrf2-ARE activation has a J-shaped dose-response: 1-way ANOVA

Chemical-specific reductions in ARE activation level measured at each of seven lower concentrations are approximately equal

Mea-sure	$\log_{10}C_i$, for i =	Chemical$_j$, for j =										
		1	2	3	4	5	6	7	8	9	All	p_{adj}
Mean	1	-3.00	-0.750	1.67	-1.18	-3.15	-0.230	-1.73	0.080	-1.91	-1.13	0.67
Mean	2	-3.57	-0.730	-3.56	1.29	-1.54	-0.970	-4.07	-3.57	-1.76	-2.08	0.67
Mean	3	-4.60	-3.52	-0.68	-3.57	-5.86	-1.52	-2.28	-5.66	-5.08	-3.61	0.24
Mean	4	-2.58	-2.06	-3.00	-1.97	-1.00	-2.92	-5.75	-2.95	-3.89	-2.90	0.67
Mean	5	-4.17	-1.50	-4.84	-3.43	-3.72	-2.65	-2.71	-5.45	-3.54	-3.56	0.67
Mean	6	-2.74	-3.25	-2.55	-2.45	-2.04	0.740	-2.70	-2.30	-3.36	-2.29	0.64
Mean	7	-4.62	-2.68	-2.62	-0.630	-1.98	-1.83	-1.86	-3.60	-1.88	-2.41	0.67
Mean	8	-3.61	-1.33	0.130	-3.21	-2.17	5.99	3.99	1.58	2.46	0.510	0.0037
Mean	9	-3.51	-0.20	-0.16	-2.94	-2.63	2.48	10.5	9.33	6.72	2.29	0.0013
Mean	10	-3.44	0.720	7.53	-1.41	11.0	10.5	20.0	37.6	37.3	13.3	$<10^{-10}$
Mean	11	9.10	14.4	26.8	4.85	47.3	13.1	41.8	69.4	78.3	33.9	$<10^{-4}$
Mean	12	38.1	39.4	43.1	25.9	71.2	28.5	71.1	82.0	83.8	51.5	$<10^{-9}$

Source: Bogen, Low-dose dose-response for in vitro Nrf2-ARE activation in human HepG2 cells. *Dose-Response* 2017 (*in press*).

Nrf2-ARE activation has a J-shaped dose-response

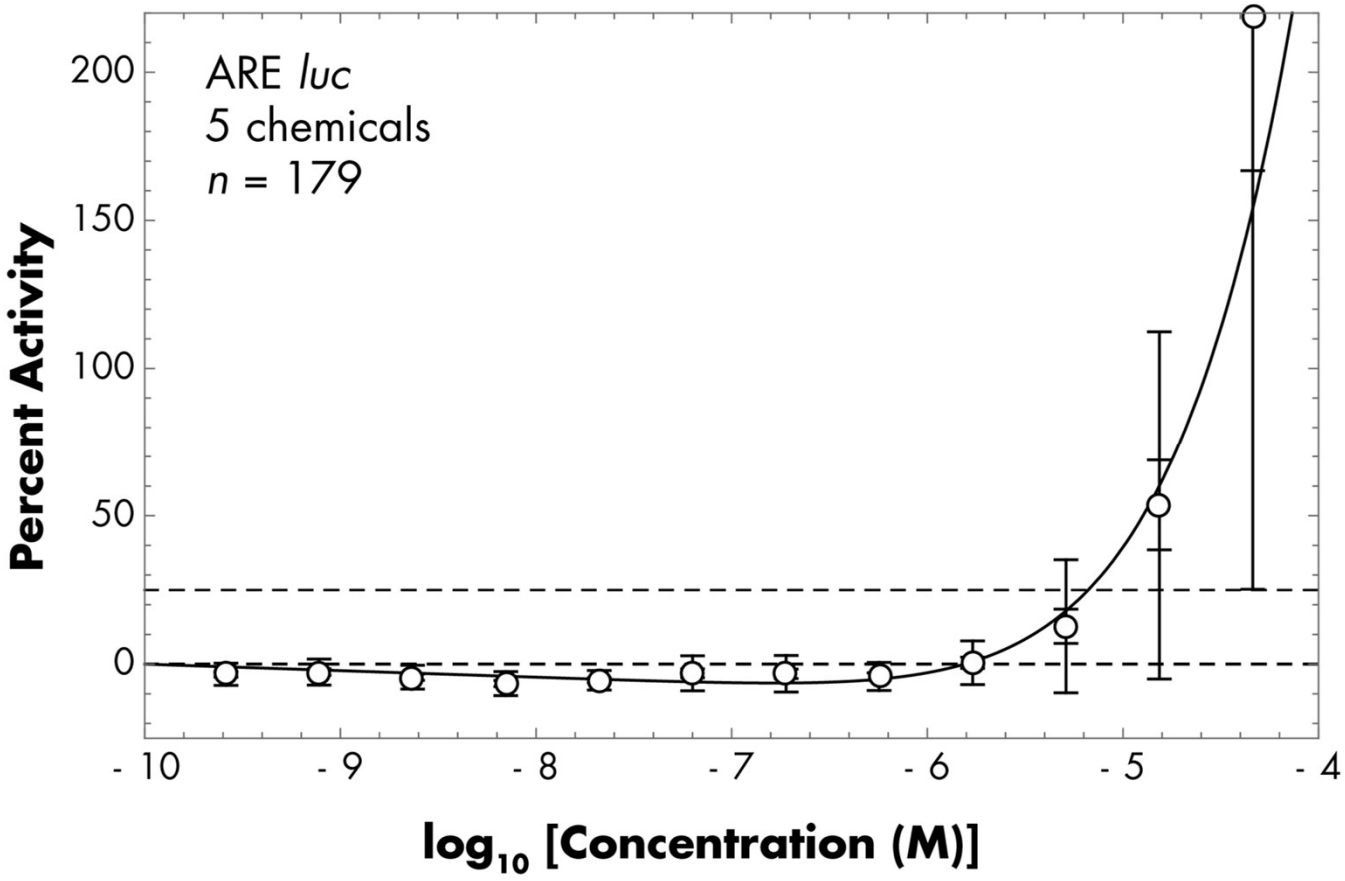

ARE-*luc in vitro* assay response relative to vehicle-exposed controls for Nrf2-ARE-pathway activation at 12 concentrations of 5 hepatotoxic chemicals.

points = arithmetic mean,
inner error bars = ±1 SDM
(outer error bars) = ±1 SD
n = total %-activity data points
dashed horizontal lines = 0%, 25% control

Fit (solid curve, $R^2 = 0.907$) includes an initial linear, **significantly negative slope** ($p = 0.00025$ by 2-tail t-test).

Source: Bogen, Low-dose dose-response for in vitro Nrf2-ARE activation in human HepG2 cells. *Dose-Response* 2017 (*in press*).

Exponent®

HSP70-repressed reduction in viability also has an (inverted) J-shaped dose-response

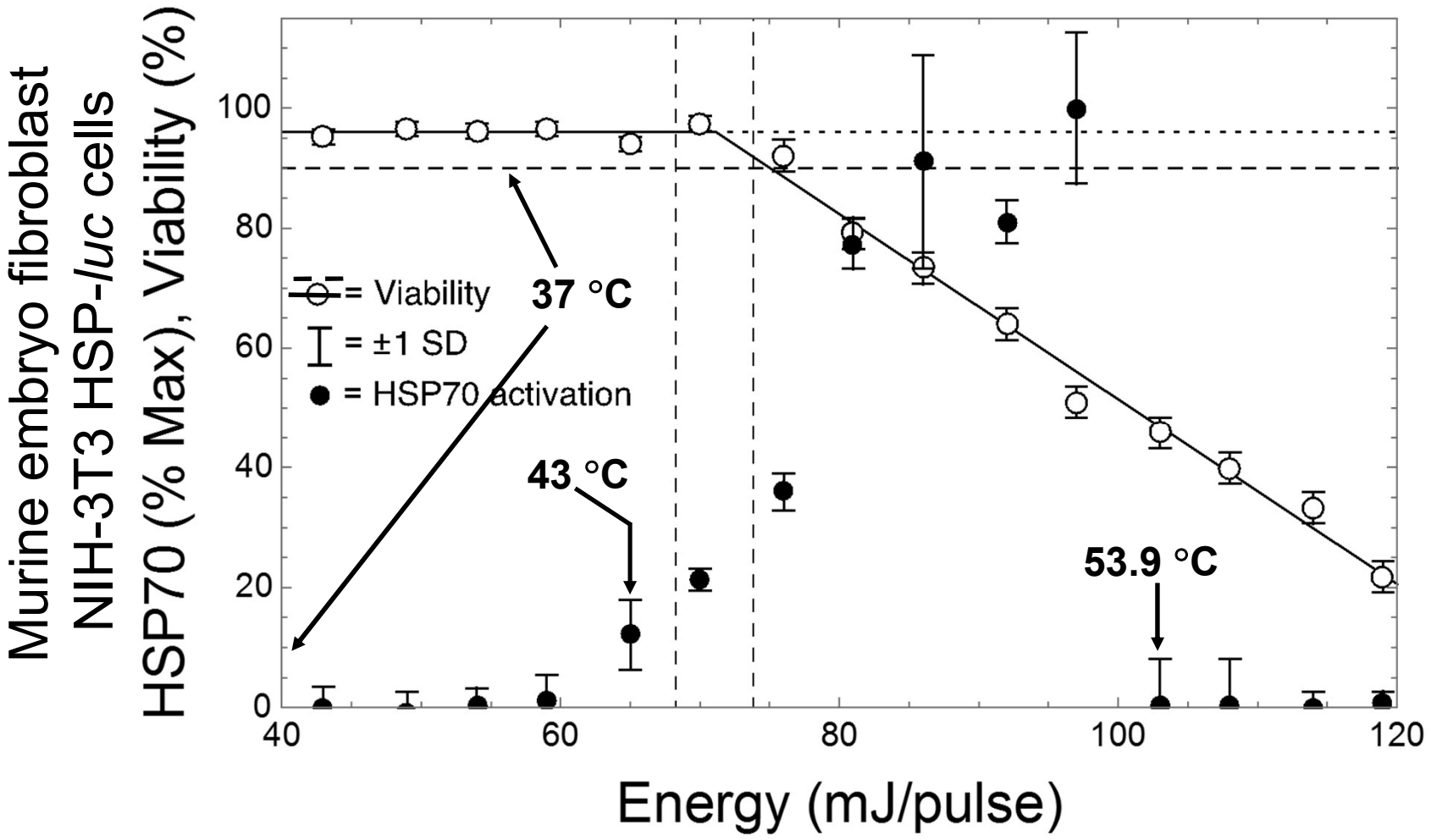

Source: Bogen, Linear-no-threshold default assumptions are unwarranted for cytotoxic endpoints independently triggered by ultrasensitive molecular switches. *Risk Analysis* 2017 (*in press*).

Conclusion

- **The dose-response of Nrf2-ARE-pathway activation in HepG2 cells is unambiguously J-shaped**

One possible interesting implication

- ***If*** **chronic, highly elevated Nrf2-ARE-pathway activation associated with chemically induced cytotoxicity and inflammation *can suffice* to drive increased tumor likelihood, then such increased risk is expected to have a *threshold-like* low-dose dose-response.**
- **This expectation would apply to *all* oxidative, ROS-generating (*including many genotoxic*) chemical carcinogens.**

Since 1976 EPA has based linear extrapolation of chemical carcinogen risks on the multistage somatic mutation (MSM) model

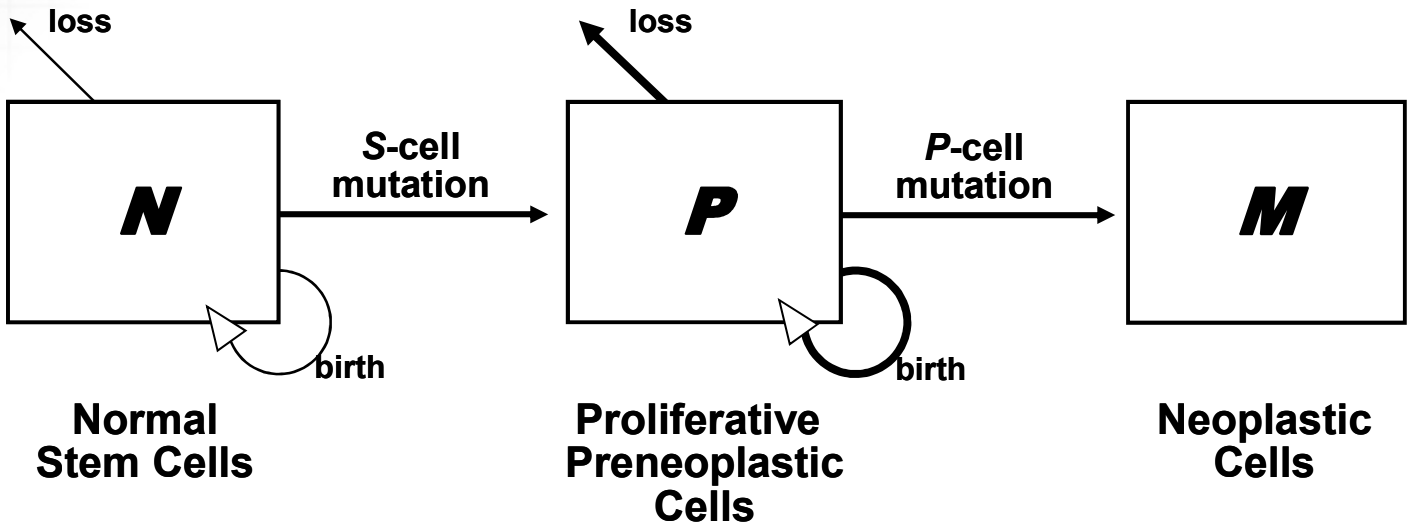

Source: Armitage & Doll 1957; Moolgavkar-Venzon-Knudsen (MVK) 1979 etc.

Data inconsistent with MSM theory

- **Many suspected oncogenes (e.g., *ras, myc*) are recessive, not dominant**
- **Cancer-cell genomes tend to accumulate 10^3–10^4 somatic mutations, and do so sporadically not gradually**
- **Cancer cells are characteristically aneuploid with translocations**
- **Deep DNA-sequencing has revealed that so many mutated-oncogene combinations occur in normal cells as to question whether they typically cause cancer** (Martincorena et al. *Science* 2015; 348(6237):880–886)

Noncoding RNA such as microRNA (miRNA) plays a key role in the emerging epigenetics biology revolution, none of which is reflected by MSM theory

- The first miRNA was discovered by Victor Ambros and his lab in 1993, in a pathway controlling development in the nematode *C. elegans*
- miRNAs were later found to be highly conserved evolutionarily in all plant and animal cells
- Ambros got the Lasker Prize in 2008 for discovering and exploring miRNA functions
- Craig Mello (from Ambros' Lab) and Andrew Fire got a Nobel Prize in 2006 for their related discovery of RNA interference

MicroRNA Biosynthesis and Action

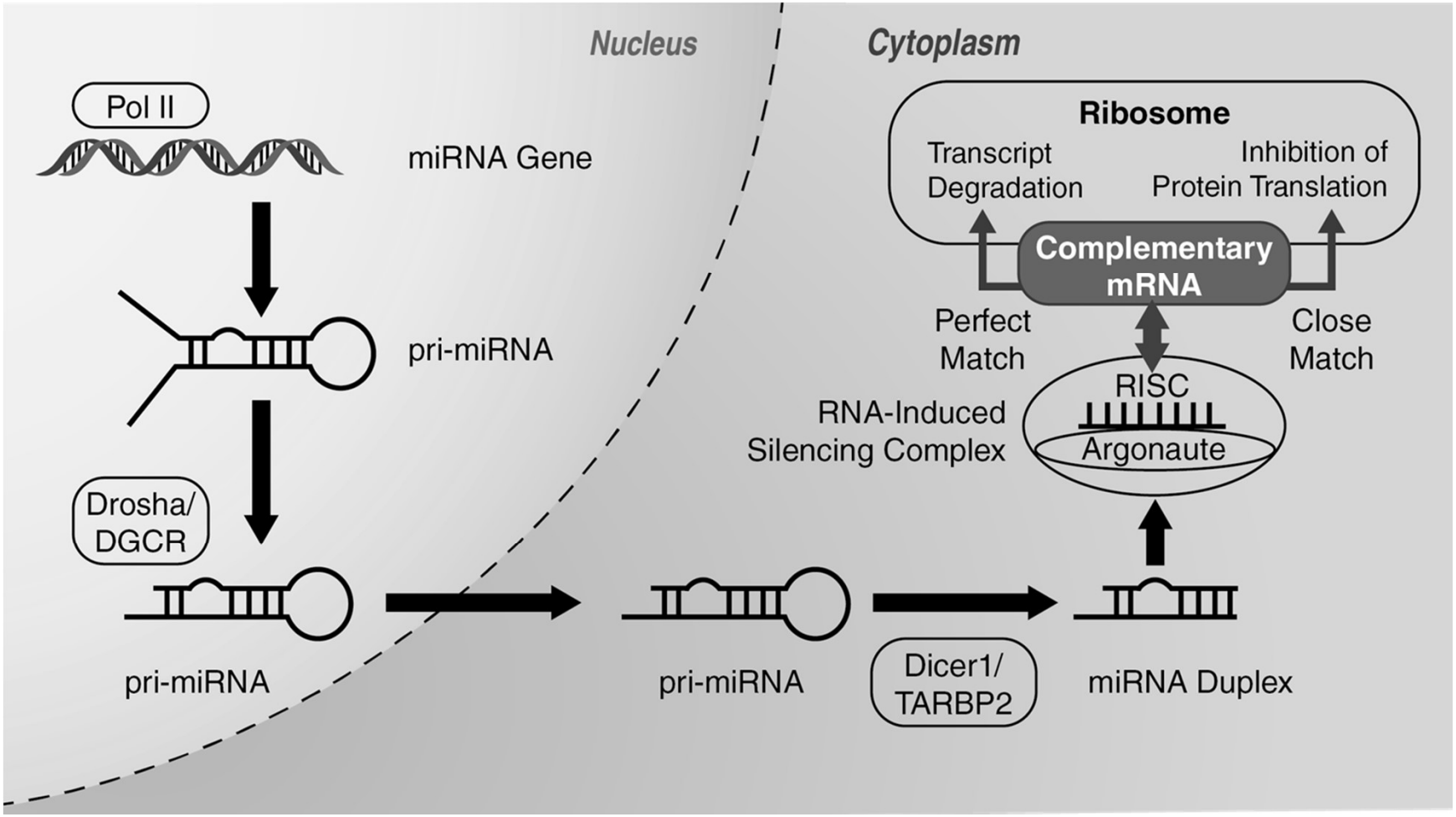

Source: Adapted from Kwan et al. *J Rad Res* 2016; Suppl ICRR Highlights:1–16.

miRNAs have Critical Regulatory Functions

- **Embryogenesis and development**
  - Tissue morphogenesis
  - Transition to and maintenance of adult phenotype
- **Adult cell and tissue responses to**
  - Stress
  - Viral, bacterial, fungal, and parasitic infections*
  - Other (cardiovascular, neoplastic) pathologies*

*See, e.g., http://www.mir2disease.org.

miRNAs Regulate the Cell Cycle

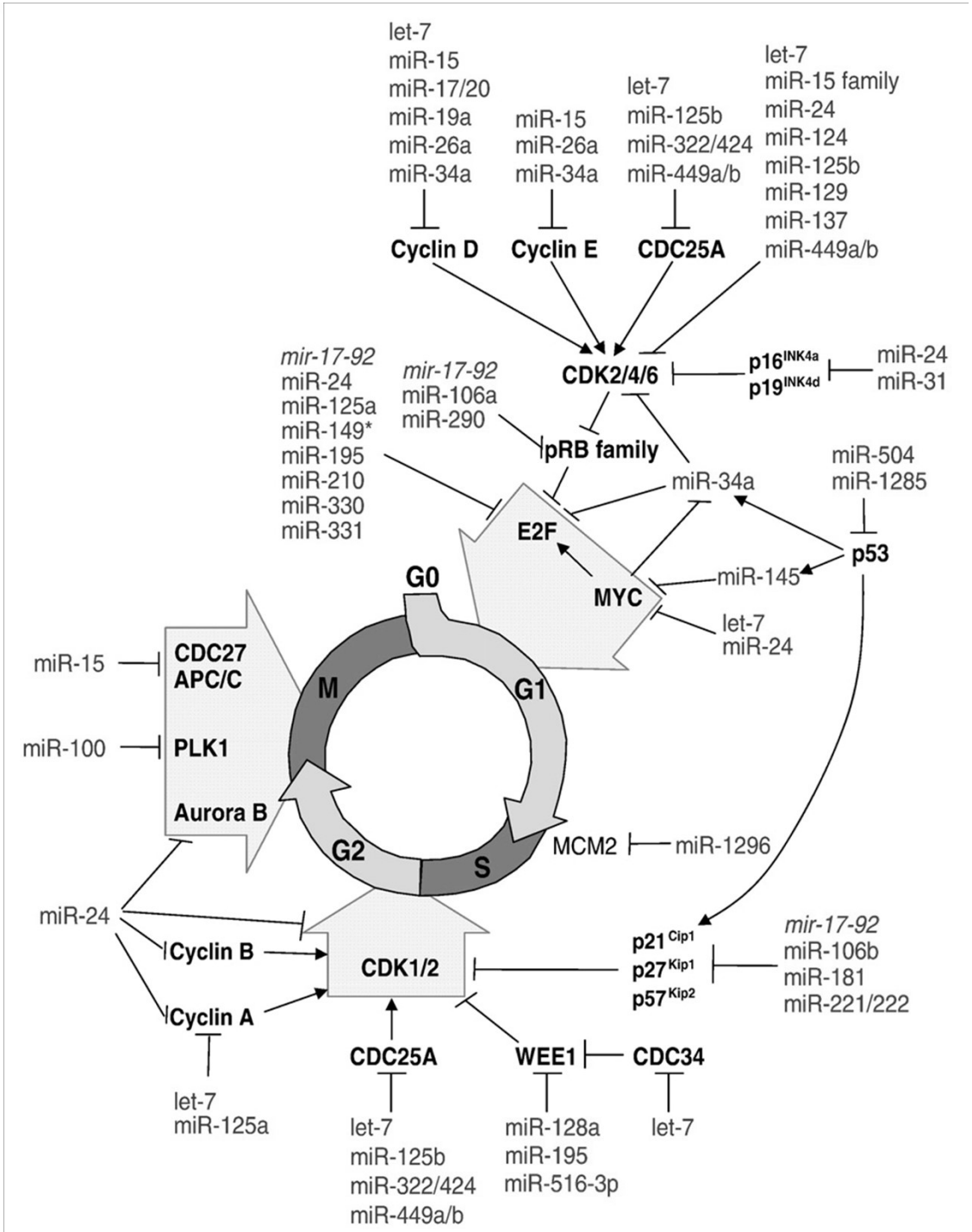

Source: Bueno & Malumbres
Biochim Biophys Acta 2011; 812:592–601.

miRNAs Regulate the Cell Cycle

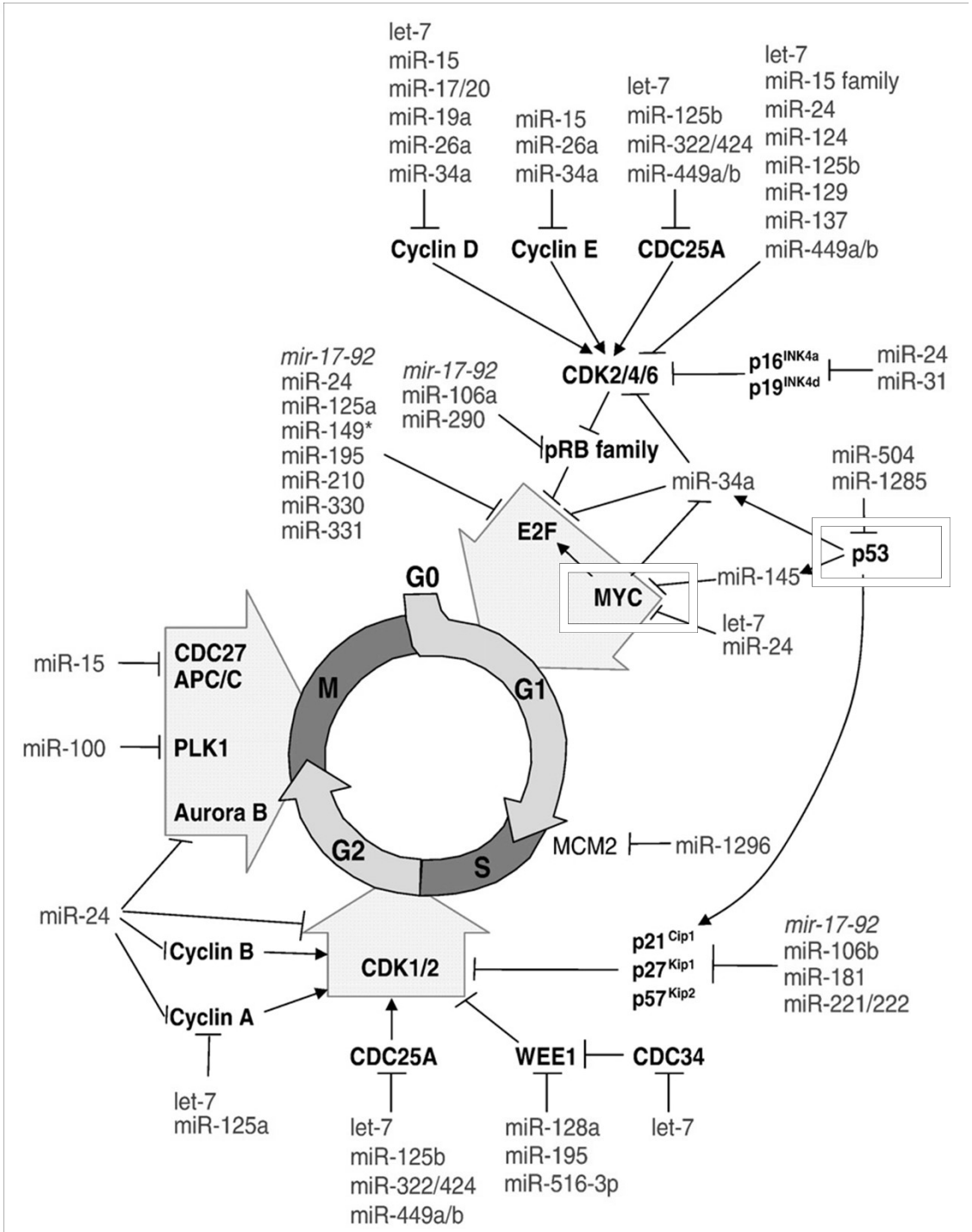

Source: Bueno & Malumbres
Biochim Biophys Acta 2011; 812:592–601.

Dysregulated miRNA profiles are specific to tumor types and tumor prognosis

miRNA	Cell cycle regulator	Down (↓), Up (↑), or De (~) -regulation in cancers
let-7 family	CDC25A, CDC34, CDK4, CDK6, Cyclin A, D1, D2, D3, c-MYC	↓ in leukemias, lymphomas, melanoma, lung, breast, gastric, gastric, pancreatic, pituitary, ovarian, kidney, prostate & colon cancer, hepatocellular carcinoma, multiple myeloma
miR-15 family (miR-15, 16, 195)	CDC27, CDK6, Cyclin D1, D3, E1, E2F3, WEE1	↓ in CLL, DLBCL, multiple myeloma, pituitary adenoma, prostate, & pancreatic cancer
miR-17 family (miR17, 20, 106, 93)	Cyclin D1, E2F1, MYCN, p21Cip1, pRb family	↑ in lung and colon cancer, lymphoma, multiple myeloma, medulloblastoma; ↓ in melanoma, ovarian & breast cancer
miR-19a	CyclinD1	~ in leukemias, hepatocellular carcinoma, colorectal & lung cancer
miR-24	AURKB, CDK1, CDK4, Cyclin A2, Cyclin B, E2F2, MYC, p16INK4a	~ in in some leukemias, hepatocellular carcinoma & prostate cancer
miR-25	p57Kip2	~ in glioblastoma, hepatocellular carcinoma, colorectar, gastric, pancreatic & prostate cancer
miR-26a	Cyclins D2 & E2	↓ in leukemia, Burkitt lymphomas, glioma, pituitary, thyroid, liver, kidney, ovarian, bladder & breast cancer
miR-31	p16INK4a, p19INK4d	~ in bladder, breast, colorectal, liver, lung, pancreatic & prostate cancer
miR-34a	CDK4, CDK6, Cyclins D1 & E2, E2F1, E2F3, c-MYC	
miR-100	PLK1	~ in bladder, ovarian, pancreatic, prostate & nasopharyngeal cancer
miR-124a	CDK6	~ in ALL, CLL, medulloblastoma, hepatocellular carcinoma, & breast, colorectal & lung cancer
miR-125b	CDC25A, CDK6, Cyclin A, E2F3	~ in neuroblastoma, medulloblastoma, liver, bladder, breast & prostate cancer
miR-128a	WEE1	~ in ALL, AML, glioblastoma, pituitary adenomas & breast cancer
miR-129	CDK6	↓ in multiple tumor cell lines & primary tumors (medulloblastoma, undifferentiated gastric cancers, lung adenocarcinoma, endometrial, ovarian and bladder cancer, & colorectal & hepatocellular carcinoma)

Dysregulated miRNA profiles are specific to tumor types and tumor prognosis *(continued)*

miRNA	Cell cycle regulator	Tumor-specific down (↓), up (↑), or de (~) -regulation
miR-145	c-MYC	~ in leukemias, Burkitt lymphomas, bladder, breast, colorectal, ovarian, gastric, lung, pancreatic, prostate cancer & hepatocellular carcinoma
miR-149*	E2F1	~ in neuroblastoma
miR-155	WEE1	~ in leukemias & lymphomas, pituitary adenomas, hepatocellular carcinoma, breast, colorectal, ovarian, lung and pancreatic cancer
miR-181 family (miR-181a, b, c)	p27Kip1	~ in leukemias, glioblastoma, hepatocellular carcinoma, breast, colorectal, lung, pancreatic & prostate cancer
miR-210	E2F3	~ in leukemias, lymphomas, glioblastoma, breast, kidney, lung, pancreatic, prostate & ovarian cancer
miR-221 family (miR-221, 222)	27Kip1, p57Kip2	~ in leukemias, glioblastoma, breast, pancreatic, prostate, ovarian, bladder, and gastric cancer, melanoma and hepatocellular carcinoma
miR-330	E2F1	↓ in follicular lymphoma, oral squamous cell carcinoma & prostate cancer
miR-331-3p	E2F1	~ in human gastric cancer
miR-322/424, miR-503	CDC25A	↓ or ~ in in some leukemias, kidney, ovarian & pancreatic cancer, and in retinoblastoma & prostate cancer
miR-449a/449b	CDC25A, CDK6	↓ in prostate cancer
miR-516a-3p	WEE1	↑ in breast cancer & in pituitary adenomas
miR-1296	MCM2	~ in prostate cancer

Source: Bueno and Malumbres *Biochim Biophys Acta* 2011; 812:592–601.

This Presentation Summarizes

A New Theory of Chemically Induced Tumorigenesis: Key Molecular Events and Dose–Response Implications

K.T. Bogen[1]
Exponent Health Sciences, Oakland, CA, United States
[1]Corresponding author: e-mail address: kbogen@exponent.com

Advances in Molecular Toxicology 2017; 10:1–54 (*in press*)
ISSN 1872-0854
http://dx.doi.org/10.1016/B978-0-12-804700-2.00001-5

ELSEVIER

AMSTERDAM • BOSTON • HEIDELBERG • LONDON
NEW YORK • OXFORD • PARIS • SAN DIEGO
SAN FRANCISCO • SINGAPORE • SYDNEY • TOKYO
Academic Press is an imprint of Elsevier

Dysregulated Adaptive Hyperplasia (DAH) theory of tumorigenesis

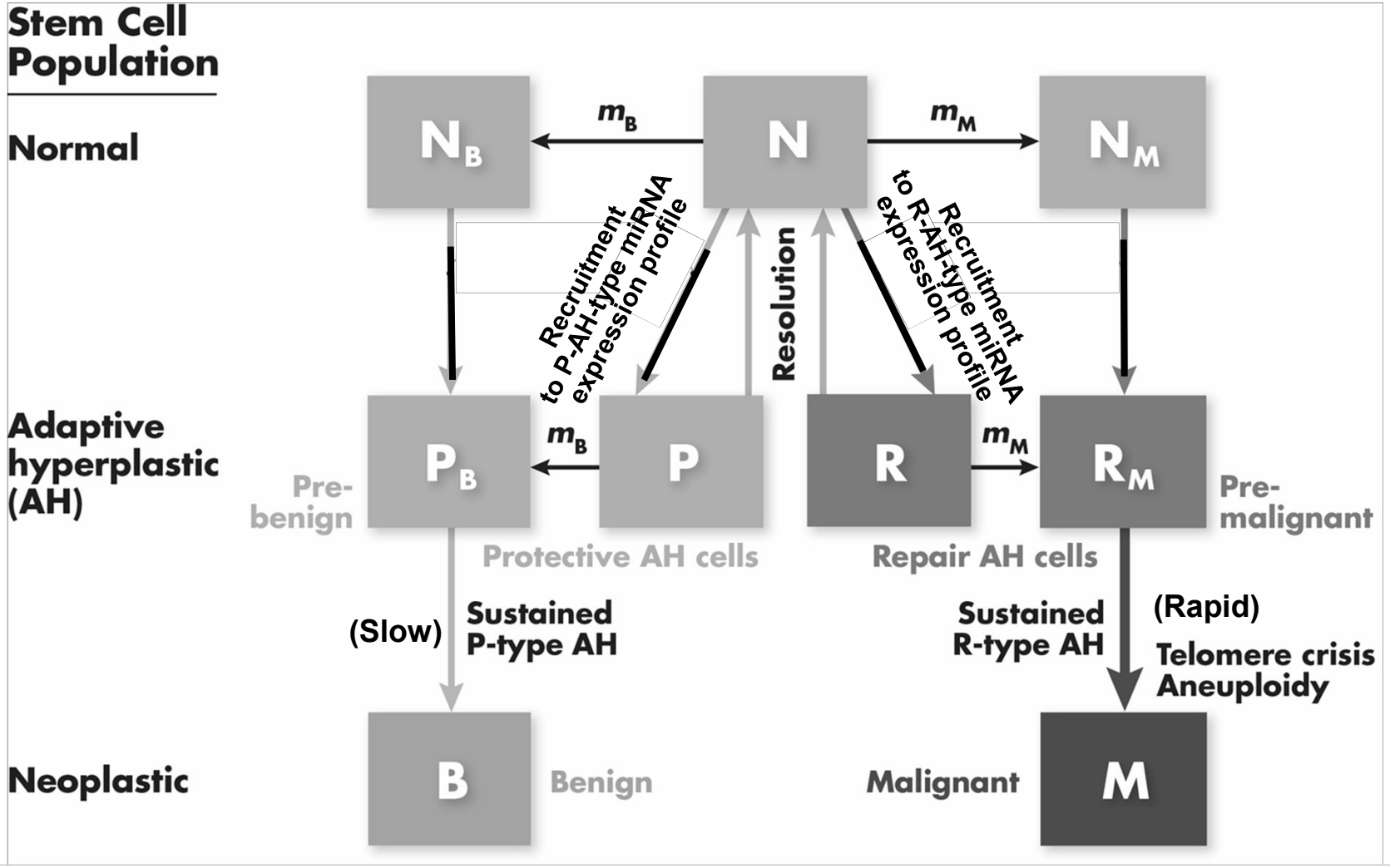

Source: Bogen *Med Hypoth* 2013; 80(1): 83–93.

Exponent®

DAH theory predicts that tumor risk is driven primarily by time-weighted average AH stem-cell number

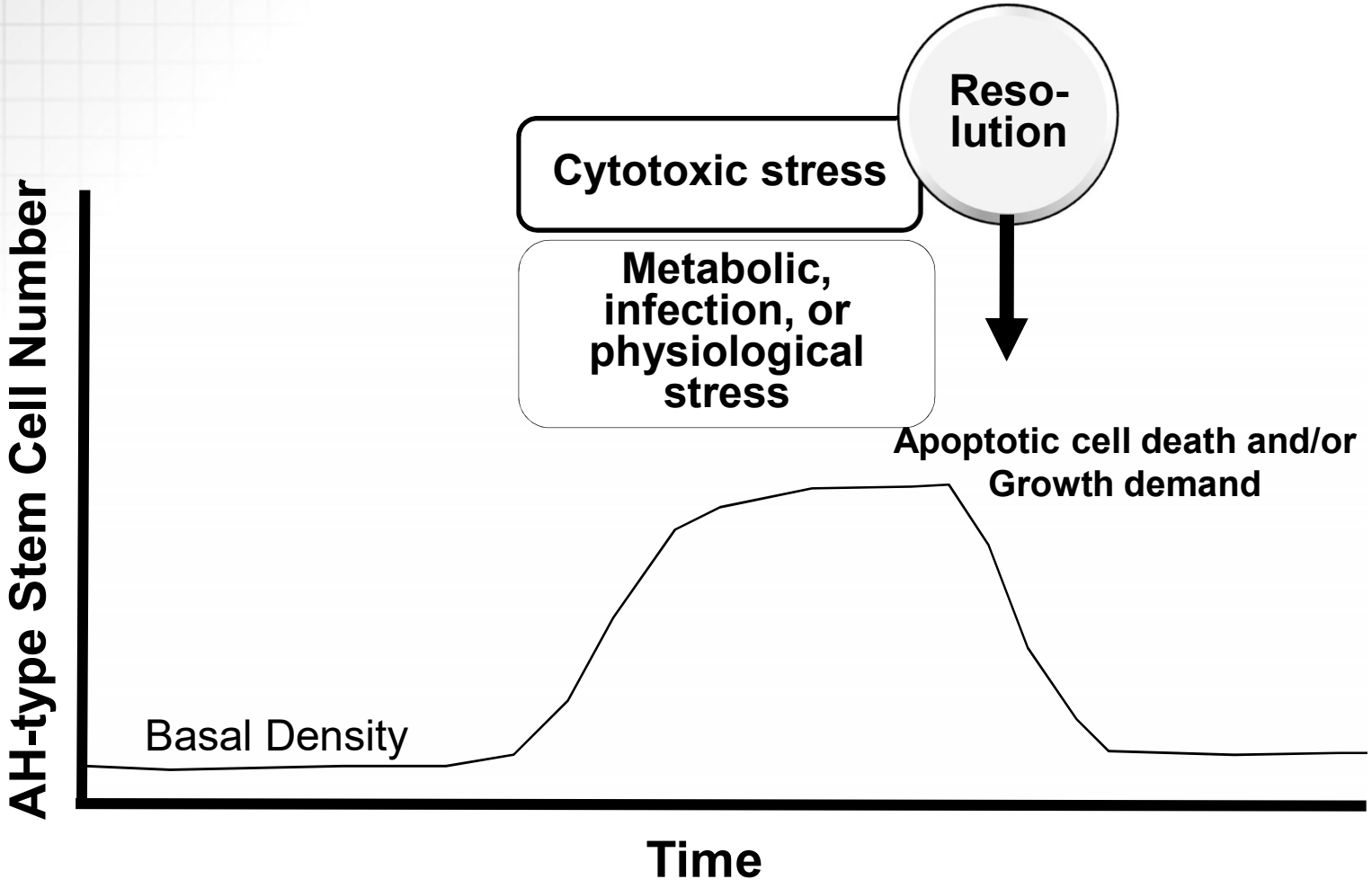

Source: Bogen *Med Hypoth* 2013; 80(1): 83–93.

Nrf2-ARE-driven DAH tumorigenesis

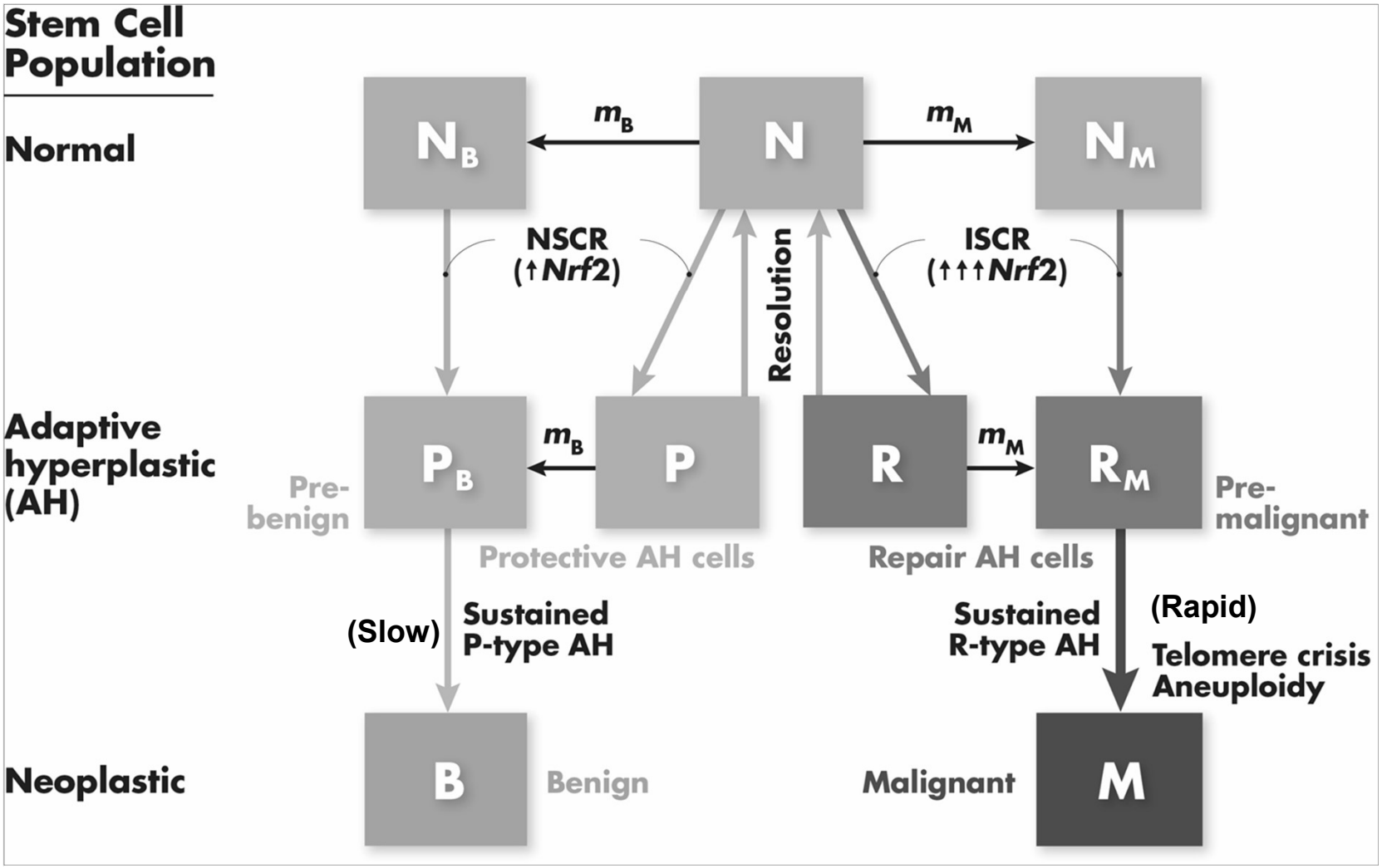

Source: Adapted from: Bogen 2017; *Adv Molec Biol* 10:1–54 (*in press*).

Exponent®

Nrf2-ARE-driven DAH tumorigenesis

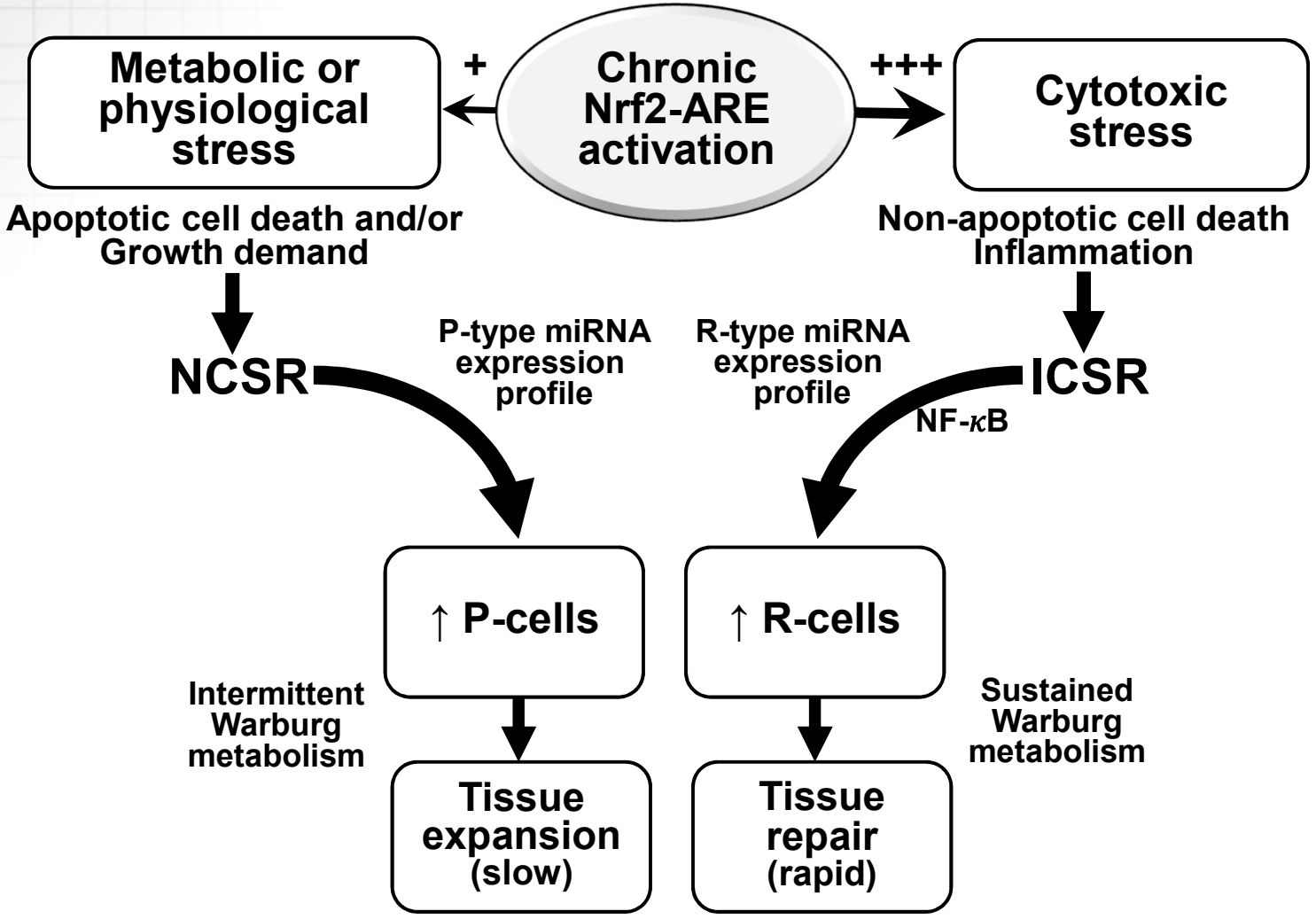

DAH theory predicts that tumor risk is driven primarily by time-weighted average AH stem-cell number

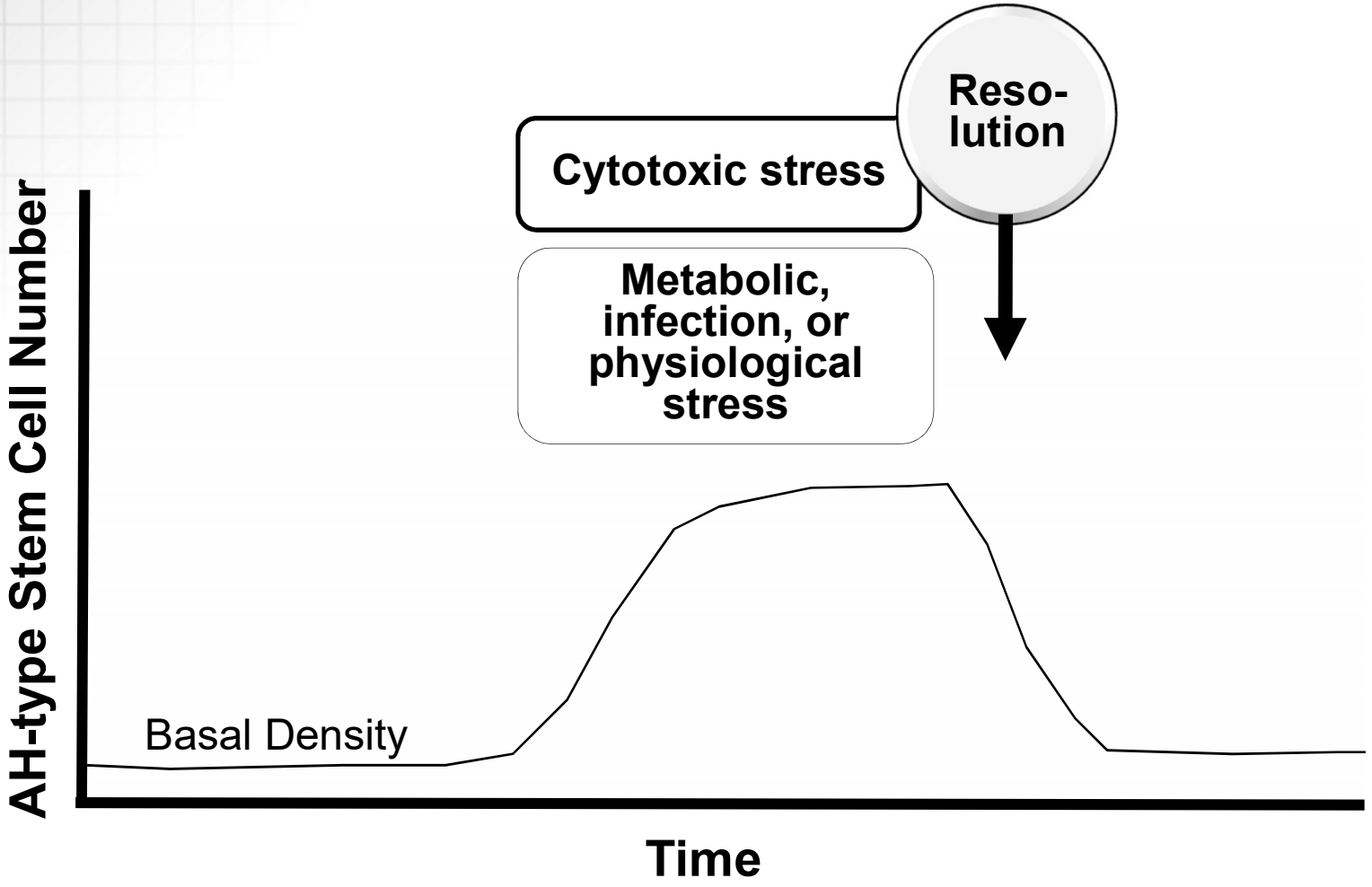

Nrf2-ARE-DAH theory also predicts that tumor risk is driven primarily by time-weighted average AH stem-cell number

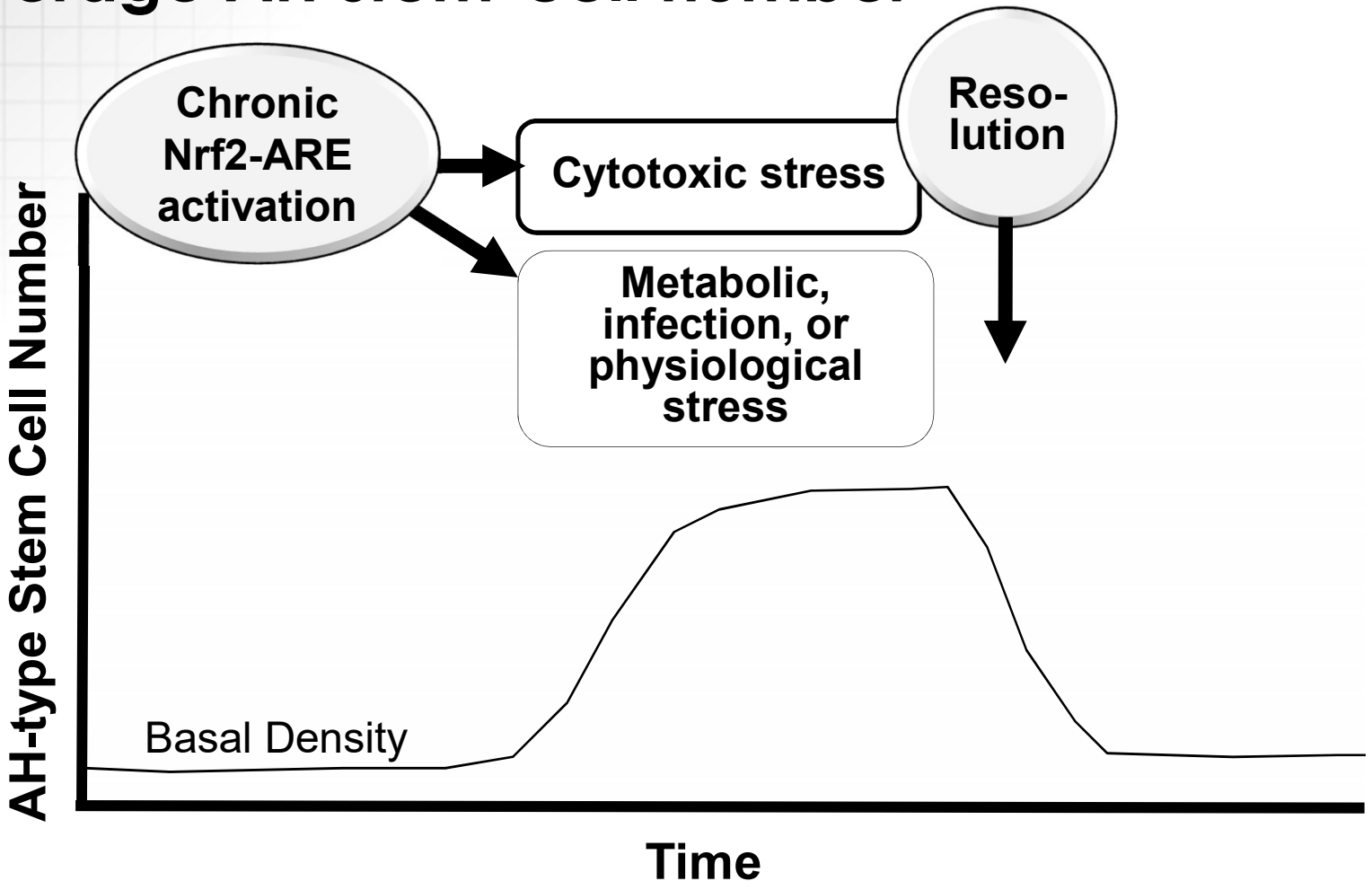

Conclusions

- The Nrf2-ARE-driven DAH model is a plausible alternative to the MSM explanation of increased tumor risks after chronic exposure to many (including genotoxic) chemical carcinogens
- This new model predicts highly nonlinear (hockey-stick-like) low-dose dose-response for increased tumor risks, driven by stem-cell recruitment into epigenetically maintained AH phenotypes
- This model can be tested by measuring tissue- and niche-specific stem cell density in relation to chemical carcinogen exposure magnitude and duration, using histochemical markers now and increasingly available for specific tissues

Additional Slides

Dose-response data inconsistent with MSM theory

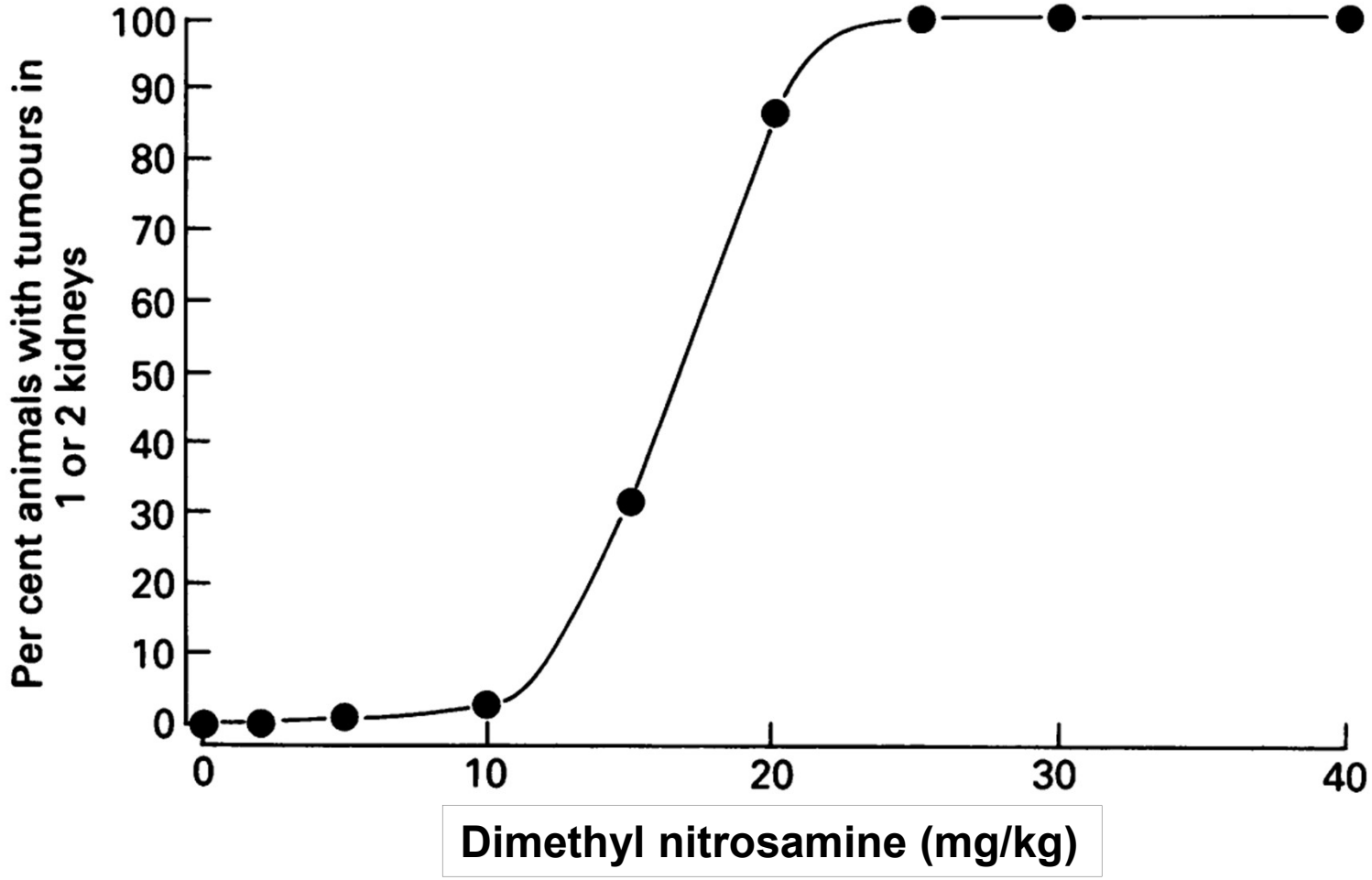

Source: Driver et al. *Br J Exp Pathol* 1987; 68:133–143.

Data not plausibly consistent with MSM theory predictions (DBP predicted to be pure promoter)

- Largest cancer bioassay ever done ("mega-trout" study of >40,000 fish)
- 9-month exposure to dibenzo[*a*,*l*]pyrene, DBP, (the most potently mutagenic carcinogen known)
- ↑ risks two tumor types *so nonlinearly* as to be consistent with MSM theory *only* if DBP is a *non-mutagenic* tumor *promoter*

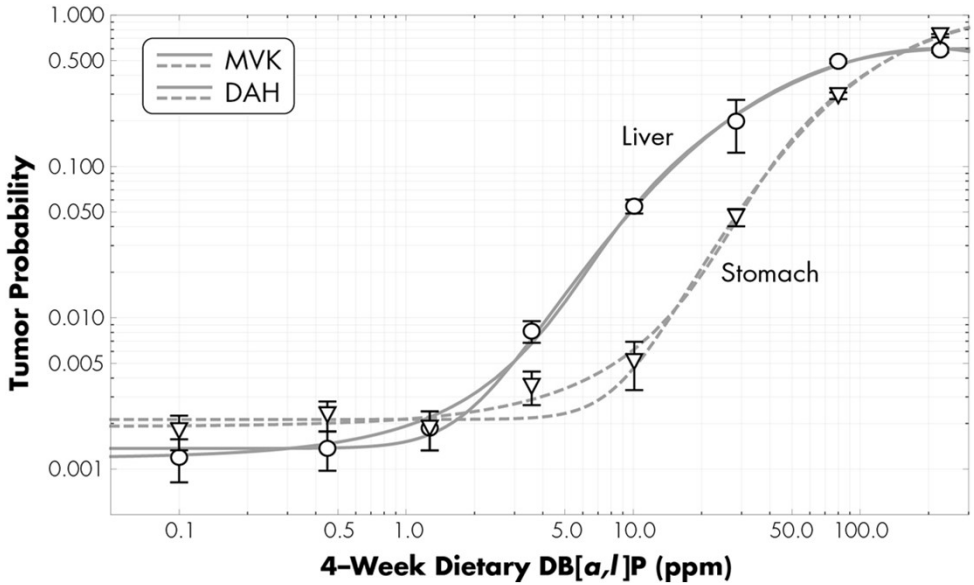

Source: Bogen *Dose-Response* 2014; 12(3):386–403.

Exponent®

Data not plausibly consistent with MSM, but consistent with DAH theory predictions

- Largest cancer bioassay ever done ("mega-trout" study of >40,000 fish)
- 9-month exposure to dibenzo[*a*,*l*]pyrene, DBP, (the most potently mutagenic carcinogen known)
- ↑ risks two tumor types *so nonlinearly* as to be consistent with MSM theory *only* if DBP is a *non-mutagenic* tumor *promoter*

DAH model ←

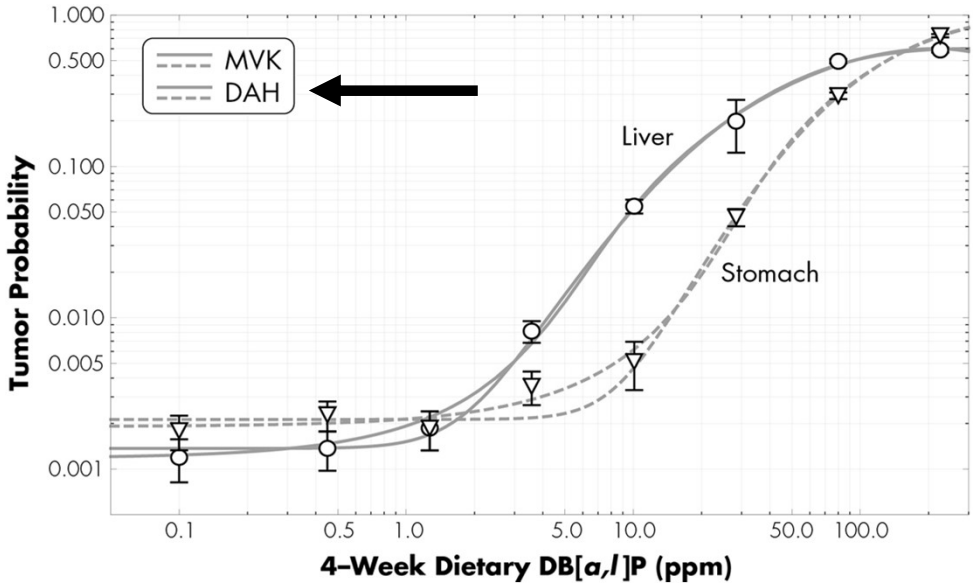

Source: Bogen *Dose-Response* 2014; 12(3):386–403.

Exponent®

Data not plausibly consistent with MSM theory predictions (DBP predicted to be pure promoter)

- Largest cancer bioassay ever done ("mega-trout" study of >40,000 fish)
- 9-month exposure to dibenzo[*a*,*l*]pyrene, DBP, (the most potently mutagenic carcinogen known)
- ↑ risks two tumor types *so nonlinearly* as to be consistent with MSM theory *only* if DBP is a *non-mutagenic* tumor *promoter*

"MVK" ←
(2-stage doubly stochastic) implementation of MSM theory

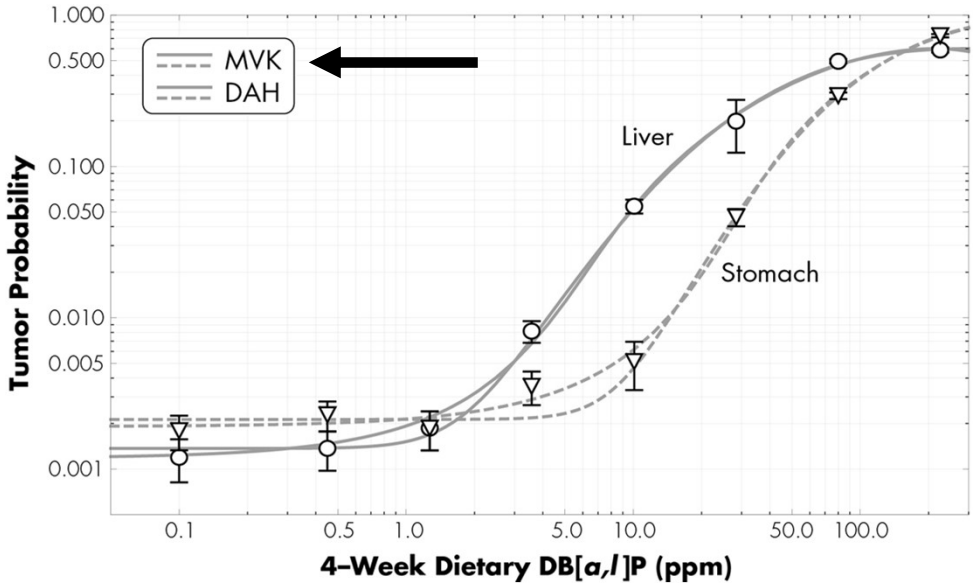

Source: Bogen *Dose-Response* 2014; 12(3):386–403.

Exponent®